US Army Corps of Engineers

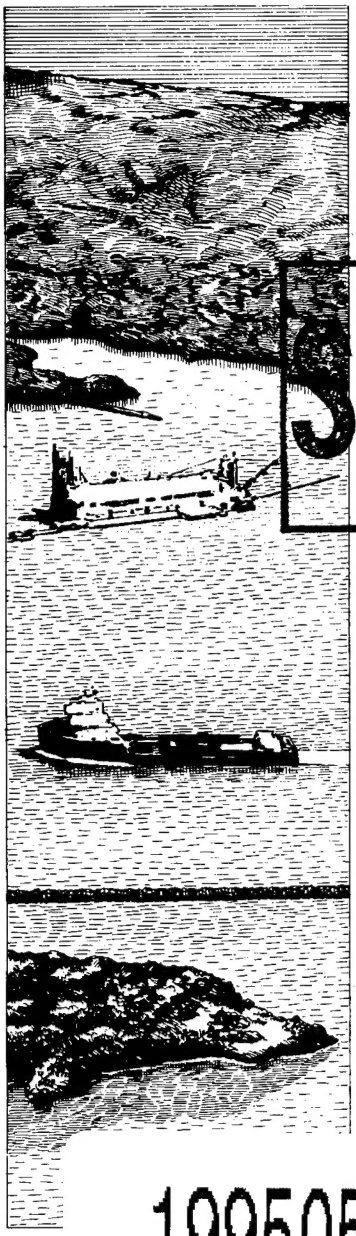

DREDGING RESEARCH PROGRAM

TECHNICAL REPORT DRP-92-6

ADCIRC: AN ADVANCED THREE-DIMENSIONAL CIRCULATION MODEL FOR SHELVES, COASTS, AND ESTUARIES

Report 6

DEVELOPMENT OF A TIDAL CONSTITUENT DATABASE FOR THE EASTERN NORTH PACIFIC

by

J. L. Hench, R. A. Luettich, Jr.

Institute of Marine Sciences
University of North Carolina at Chapel Hill
Morehead City, North Carolina 27514

J. J. Westerink

Department of Civil Engineering and Geological Sciences
University of Notre Dame
Notre Dame, Indiana 46556

N. W. Scheffner

Waterways Experiment Station, Corps of Engineers
3909 Halls Ferry Road, Vicksburg, Mississippi 39180-6199

December 1994

Report 6 of a Series

Prepared for DEPARTMENT OF THE ARMY
U.S. Army Corps of Engineers
Washington, DC 20314-1000

The Dredging Research Program (DRP) is a seven-year program of the US Army Corps of Engineers. DRP research is managed in these five technical areas:

Area 1 - Analysis of Dredged Material Placed in Open Waters

Area 2 - Material Properties Related to Navigation and Dredging

Area 3 - Dredge Plant Equipment and Systems Processes

Area 4 - Vessel Positioning, Survey Controls, and Dredge Monitoring Systems

Area 5 - Management of Dredging Projects

US Army Corps
of Engineers
Waterways Experiment
Station

Dredging Research Program Report Summary

ADCIRC: An Advanced Three-Dimensional Circulation Model for Shelves, Coasts, and Estuaries; Report 6, Development of a Tidal Constituent Database for the Eastern North Pacific (TR DRP-92-6)

ISSUE: Dredged-material disposal sites located in open water are classified as either dispersive or nondispersive depending on whether local water velocities are strong enough to erode and transport dredged material from the deposited mound. The Corps needs the capability to predict stability of the mound and long-term migration patterns of eroded material to (1) identify acceptable disposal-site locations, and (2) provide a quantitative approach for gaining site-designation approval.

RESEARCH: The overall work-unit objective is development of a systematic approach for predicting the dispersion characteristics of a specific open-water disposal site. This objective includes the following goals:

- Identify realistic wind-, wave-, tide-, and storm-generated velocity boundary conditions.
- Develop numerical models capable of simulating dispersion characteristics of dredged-material mounds for periods of time in excess of one year.
- Provide site-designation technology to field engineers as a tool in site identification and designation.

This study reports the tidal-constituent database developed for locations along the eastern North Pacific coast of the United States, which is a part of the first two goals listed above.

SUMMARY: The numerical model ADCIRC-2DDI (a two-dimensional depth-averaged barotropic hydrodynamic model) was applied to the eastern North Pacific to develop a tidal constituent database. The report includes the specification of a geometrically and hydrodynamically simple open boundary, the use of large domains, and the advantages of using a graded finite element grid to selectively resolve flow features of interest.

AVAILABILITY OF REPORT: The report is available through the Interlibrary Loan Service from the U.S. Army Engineer Waterways Experiment Station (WES) Library, telephone number (601) 634-2355. National Technical Information Service (NTIS) report numbers may be requested from WES Librarians.

To purchase a copy of the report, call NTIS at (703) 487-4780.

About the Authors: Dr. J. L. Hench and Dr. R. A. Luettich, Jr., are members of the Institute of Marine Sciences, University of North Carolina at Chapel Hill; Dr. J. J. Westerink, Department of Civil Engineering and Geological Sciences of the University of Notre Dame; and Dr. Norman W. Scheffner, the Coastal Engineering Research Center.

Point of Contact: Dr. Scheffner, Principal Investigator for the work unit. For further information about the DRP, contact Mr. E. Clark McNair, Jr., Manager, DRP, at (601) 634-2070.

Dredging Research Program

Technical Report DRP-92-6
December 1994

ADCIRC: An Advanced Three-Dimensional Circulation Model for Shelves, Coasts, and Estuaries

Report 6
Development of a Tidal Constituent Database for the Eastern North Pacific

by J. L. Hench, R. A. Luettich, Jr.
Institute of Marine Sciences
University of North Carolina at Chapel Hill
Morehead City, NC 27514

J. J. Westerink

Department of Civil Engineering and Geological Sciences
University of Notre Dame
Notre Dame, IN 46556

N. W. Scheffner

U.S. Army Corps of Engineers
Waterways Experiment Station
3909 Halls Ferry Road
Vicksburg , MS 39180-6199

Report 6 of a series

Approved for public release; distribution is unlimited

Prepared for U.S. Army Corps of Engineers
Washington, DC 20314-1000

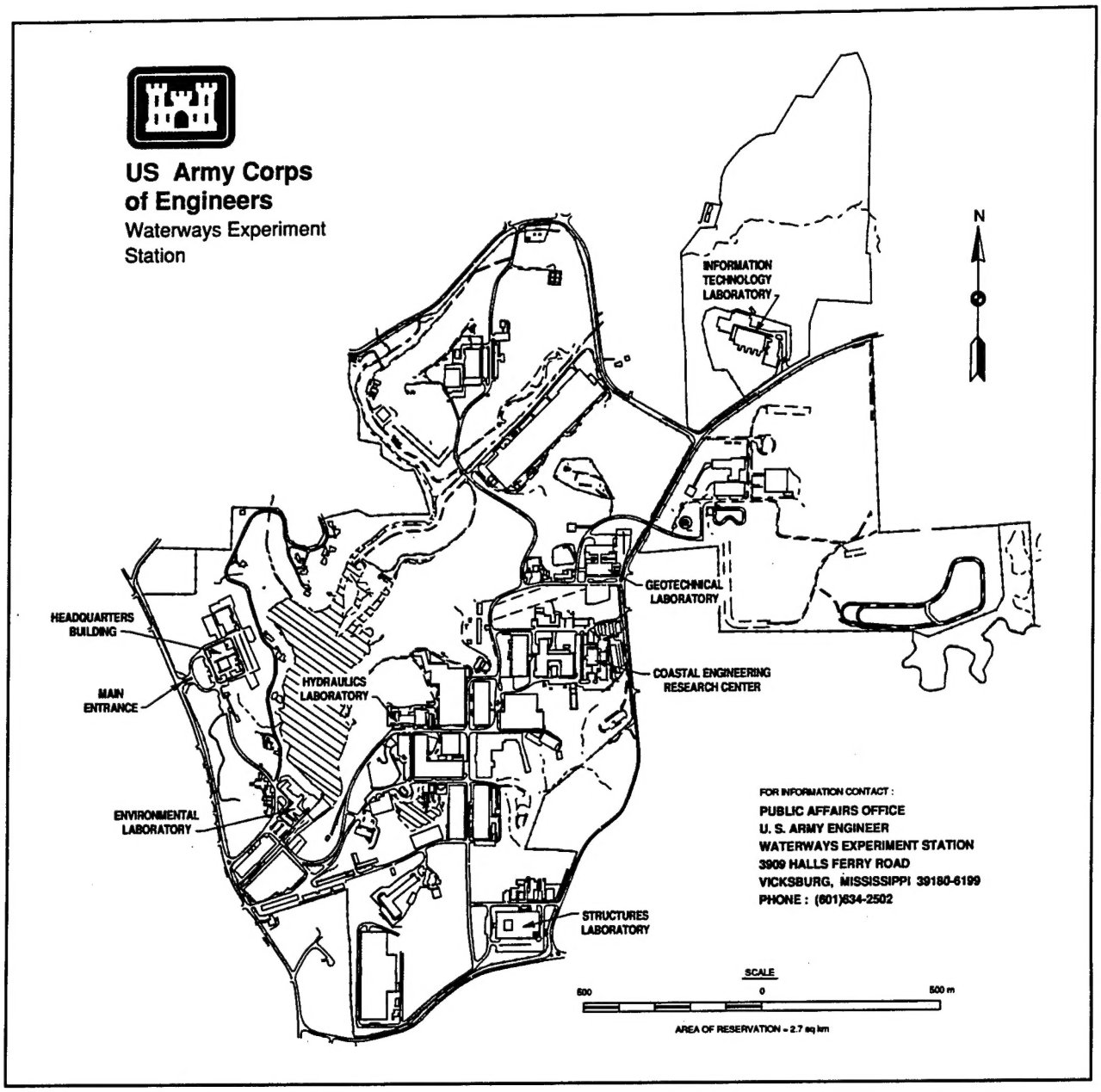

Waterways Experiment Station Cataloging-in-Publication Data

ADCIRC : an advanced three-dimensional circulation model for shelves, coasts, and estuaries. Report 6, Development of a tidal constituent database for the eastern North Pacific / by J.L. Hench ... [et al.] ; prepared for U.S. Army Corps of Engineers.

60 p. : ill. ; 28 cm. — (Technical report ; DRP-92-6 rept. 6)

Includes bibliographical references.

Report 6 of a series.

1. Tides — North Pacific Ocean — Databases. 2. Tide-predictors — Mathematical models. 3. Ocean circulation — North Pacific Ocean — Mathematical models. 4. Hydrodynamics — Mathematical models. I. Hench, J. L. II. United States. Army. Corps of Engineers. III. U.S. Army Engineer Waterways Experiment Station. IV. Dredging Research Program. V. Title: An advanced three-dimensional circulation model for shelves, coasts, and estuaries. VI. Title: Development of a tidal constituent database for the eastern North Pacific. VII. Series: Technical report (U.S. Army Engineer Waterways Experiment Station) ; DRP-92-6 rept. 6.

TA7 W34 no.DRP-92-6 rept. 6

Contents

Preface

The research described in this report was authorized and funded under Work Unit 32466, "Numerical Simulation Techniques for Evaluating Long-Term Fate and Stability of Dredged Material Disposed in Open Water," of Technical Area 1 (TA1), "Analysis of Dredged Material Placed in Open Water," of the Dredging Research Program (DRP). The DRP is sponsored by Headquarters, U.S. Army Corps of Engineers (HQUSACE). Administrative responsibility is assigned to the U.S. Army Engineer Waterways Experiment Station (WES) Coastal Engineering Research Center (CERC), Dr. James R. Houston, Director, and Mr. Charles C. Calhoun, Jr., Assistant Director.

Mr. John H. Lockhart, Jr., HQUSACE, was DRP TA1 Technical Monitor. Mr. E. Clark McNair, Jr., was DRP Program Manager (PM), and Dr. Lyndell Z. Hales was assistant PM. Dr. Billy H. Johnson, Senior Research Hydraulic Engineer, was the TA1 Technical Area Manager, and Dr. Norman W. Scheffner, Research Division (RD), CERC, was the Principal Investigator for the work unit. Dr. Scheffner worked under the administrative supervision of Mr. H. Lee Butler, Chief, RD, CERC.

This study was performed and the report was prepared over the period 1 September 1993 through 15 August 1994. The numerical modeling goals, concepts, and methodology were developed by Dr. Scheffner and two DRP contractors: Dr. Joannes J. Westerink of the University of Notre Dame and Dr. Richard A. Luettich, Jr., of the University of North Carolina at Chapel Hill. Development and implementation of the model were completed by Drs. Westerink and Luettich and Mr. James L. Hench of the University of North Carolina at Chapel Hill.

At the time of publication of this report, Director of WES was Dr. Robert W. Whalin. Commander was COL Bruce K. Howard, EN.

Additional information on this report can be obtained from Mr. E. Clark McNair, Jr., DRP Program Manager, at (601) 634-2070 or Dr. Norman W. Scheffner, Principal Investigator, at (601) 634-3220.

Summary

This report describes the application of ADCIRC-2DDI, a two-dimensional, depth-averaged, barotropic hydrodynamic model, to the eastern North Pacific in order to develop a tidal constituent database. Issues that are emphasized in the development of the Eastern North Pacific Tidal (ENPACT) model include the specification of a geometrically and hydrodynamically simple open boundary, the use of large domains, and the advantages of using a graded finite element grid to selectively resolve flow features of interest.

The ENPACT model is coupled to a finite element global ocean model at the open boundary and forced with five diurnal and semidiurnal astronomical tidal constituents (K_1, O_1, M_2, S_2, and N_2). Tidal potential forcing is applied to the interior of the domain for the same constituents. The structures of the various tides are examined and the results of the tidal simulations are compared with field data at 72 fixed tidal elevation stations.

1 Introduction

This report presents the initial results from a numerical tidal model of the eastern North Pacific which encompasses the coastal ocean as well as the deep open ocean. The simulations were performed using ADCIRC-2DDI, a two-dimensional depth-integrated barotropic finite element hydrodynamic code.

The Eastern North Pacific Tidal (ENPACT) model is intended to provide a bridge between global ocean models which are adequate for the deep ocean but poorly resolve shelf and nearshore areas, and small domain coastal models (e.g., Flather 1987, Forman et al. 1993) which adequately resolve the nearshore features but can suffer from poor open boundary conditions, particularly from the higher harmonics which are generated on the shelf. The results of this model are intended to provide a tidal constituent database from which accurate boundary conditions can be extracted to drive smaller localized models with higher resolution. In earlier work, a similar database was generated for the entire western North Atlantic using the same code (see Westerink, Luettich, and Scheffner 1993).

Issues emphasized in this report include the use of a geometrically and hydrodynamically simple open boundary, the use of a large computational domain in order to accurately propagate tides from the deep ocean onto the shelf, and the use of a graded finite element grid to reduce computational overhead. Model results are compared with observational data at 72 fixed-elevation recording stations distributed throughout the domain.

The size of the ENPACT model domain is nearly 2×10^7 sq km and would be computationally prohibitive to discretize in a uniform manner at the resolution required to resolve the rapidly varying flow features on the shelf. Much of the domain lies in the deep ocean, which requires only relatively coarse resolution since the tides vary so slowly there. Therefore, a graded finite mesh was designed to minimize the size of the discrete problem, while still resolving the flow features of interest.

The remainder of this report discusses the application of ADCIRC-2DDI to simulate astronomical tides in the eastern North Pacific. Chapter 2 gives a brief summary of the formulation and numerical discretization of the model. Chapter 3 describes the computational domain and the modeling strategy. Chapter 4 details the model runs. In Chapter 5, comparisons between modeled

and observed tidal elevations are made. Chapters 5 and 6 provide discussion and conclusions for this study. Finally, Appendix A outlines procedures for resynthesizing harmonic constituents for model results and field data.

2 Governing Equations and Numerical Discretization

The computations described in this report were performed using ADCIRC-2DDI, the depth-integrated version of a group of two- and three-dimensional hydrodynamic codes named ADCIRC. A full treatment of the governing equations and the numerical techniques used in ADCIRC is given in Luettich, Westerink, and Scheffner (1992). The following briefly outlines their derivation and numerical discretization. ADCIRC-2DDI uses the depth-integrated equations of mass and momentum conservation, subject to the incompressibility, Boussinesq, and hydrostatic pressure approximations. Using the standard quadratic parameterization for bottom stress and neglecting baroclinic terms and lateral diffusion/dispersion effects leads to the following set of conservation statements in primitive non-conservative form expressed in a spherical coordinate system (Flather 1988, Kolar et al. 1994):

$$\frac{\partial \zeta}{\partial t} + \frac{1}{R\cos\varphi}\left[\frac{\partial UH}{\partial \lambda} + \frac{\partial (VH\cos\varphi)}{\partial \varphi}\right] = 0 \tag{1}$$

$$\frac{\partial U}{\partial t} + \frac{1}{R\cos\varphi}U\frac{\partial U}{\partial \lambda} + \frac{1}{R}V\frac{\partial U}{\partial \varphi} - \left(\frac{\tan\varphi}{R}U + f\right)V = - \frac{1}{R\cos\varphi}\frac{\partial}{\partial \lambda}\left[\frac{P_s}{\rho_0} + g(\zeta - \eta)\right] + \frac{\tau_{s\lambda}}{\rho_o H} - \tau_* V \tag{2}$$

$$\frac{\partial V}{\partial t} + \frac{1}{R\cos\varphi}U\frac{\partial V}{\partial \lambda} + \frac{1}{R}V\frac{\partial V}{\partial \varphi} - \left(\frac{\tan\varphi}{R}U + f\right)U = - \frac{1}{R}\frac{\partial}{\partial \varphi}\left[\frac{p_s}{\rho_0} + g(\zeta - \eta)\right] + \frac{\tau_{s\varphi}}{\rho_o H} - \tau_* V \tag{3}$$

where

ζ = free surface elevation relative to the geoid

t = time

R = radius of the earth

λ, φ = degrees longitude (east of Greenwich positive) and degrees latitude (north of the equator positive)

U, V = depth-averaged horizontal velocities

$H = \zeta + h$ = total water column

h = bathymetric depth relative to the geoid

$f = 2\Omega sin\ \varphi =$ Coriolis parameter

Ω = angular speed of the earth

p_s = atmospheric pressure at the free surface

ρ_0 = reference density of water

g = acceleration due to gravity

η = effective Newtonian equilibrium tide potential

$\tau_{s\lambda}$, $\tau_{s\varphi}$ = applied free surface stress

$$\tau_* = C_f \frac{(U^2 + V^2)^{1/2}}{H}$$

C_f = bottom friction coefficient

A practical expression for the effective Newtonian equilibrium tide potential is given by Reid (1990) as:

$$\eta(\lambda,\varphi,t) = \sum_{n,\ j} \alpha_{jn} C_{jn} f_{jn}(t_0) L_j(\varphi) \cos\left[\frac{2\pi(t - t_0)}{T_{jn} + j\lambda + v_{jn}(t_0)}\right] \qquad (4)$$

where

λ,φ = degrees longitude and latitude, respectively

α_{jn} = effective earth elasticity factor for tidal constituent n of species j

C_{jn} = constant characterizing the amplitude of tidal constituent n of species j

f_{jn} = time-dependent nodal factor

$j = 0,1,2$ = tidal species ($j = 0$, declinational; $j = 1$, diurnal; $j = 2$, semidiurnal)

t_0 = reference time

T_{jn} = period of constituent n of species j

v_{jn} = time-dependent astronomical argument

$L_0 = 3\sin^2 \varphi - 1$

$L_1 = \sin(2\varphi)$

$L_2 = \cos^2(\varphi)$

Values for C_{jn} are presented by Reid (1990). The value for the effective earth elasticity factor, α_{jn}, is typically taken as 0.69 for all tidal constituents (Schwiderski 1980, Hendershott 1981) although its value has been shown to be slightly constituent dependent (Wahr 1981, Woodworth 1990).

To facilitate a finite element (FE) solution to Equations 1-3, these equations are mapped from spherical form onto a rectilinear coordinate system using a Carte Parallelogrammatique (CP) projection (Pearson 1990):

$$x' = R(\lambda - \lambda_0)\cos\varphi_0 \tag{5}$$

$$y' = R\varphi \tag{6}$$

where λ_0, φ_0 = center point of the projection. Applying the CP projection to Equations 1-3 gives the shallow-water equations in primitive nonconservative form expressed in the CP coordinate system:

$$\frac{\partial \zeta}{\partial t} + \frac{\cos\varphi_0}{\cos\varphi}\frac{\partial (UH)}{\partial x'} + \frac{1}{\cos\varphi}\frac{\partial (VH\cos\varphi)}{\partial y'} = 0 \tag{7}$$

$$\frac{\partial U}{\partial t} + \frac{\cos\varphi_0}{\cos\varphi} U \frac{\partial U}{\partial x'} + V \frac{\partial U}{\partial y'} - \left(\frac{\tan\varphi}{R} U + f \right) V$$
$$= - \frac{\cos\varphi_0}{\cos\varphi} \frac{\partial}{\partial x'} \left[\frac{p_s}{\rho_0} + g(\zeta - \eta) \right] + \frac{\tau_{s\lambda}}{\rho_0 H} - \tau_* U \tag{8}$$

$$\frac{\partial V}{\partial t} + \frac{\cos\varphi_0}{\cos\varphi} U \frac{\partial V}{\partial x'} + V \frac{\partial V}{\partial y'} - \left(\frac{\tan\varphi}{R} U + f \right) U$$
$$= - \frac{\partial}{\partial y'} \left[\frac{p_s}{\rho_0} + g(\zeta - \eta) \right] + \frac{\tau_{s\varphi}}{\rho_0 H} - \tau_* V \tag{9}$$

Utilizing the FE method to resolve the spatial dependence in the shallow-water equations in their primitive form chronically gives inaccurate solutions with severe artificial near $2 \cdot \Delta x$ modes (Gray 1982). However, reformulating the primitive equations into a generalized wave continuity wave equation (GWCE) gives highly accurate, noise-free, FE-based solutions to the shallow-water equations (Lynch and Gray 1979, Kinnmark 1984). The GWCE is derived by taking the time derivative of the primitive continuity equation and spatial derivatives of the primitive horizontal momentum equations. The spatially differentiated primitive horizontal momentum equations are then substituted into the time-differentiated primitive continuity equation, which in turn is added to the original primitive continuity equation multiplied by a constant in space and time, τ_0 (Lynch and Gray 1979; Kinnmark 1984; Luettich, Westerink, and Scheffner 1992). After applying the CP coordinate projection, the GWCE is:

$$\frac{\partial^2 \zeta}{\partial t^2} + \tau_0 \frac{\partial \zeta}{\partial t} + \frac{\cos\varphi_0}{\cos\varphi} \frac{\partial}{\partial x'} \frac{\partial \zeta}{\partial t} \left\{ U - \frac{\cos\varphi_0}{\cos\varphi} UH \frac{\partial U}{\partial x'} - VH \frac{\partial U}{\partial y'} \right.$$
$$+ \left(\frac{\tan\varphi}{R} U + f \right) VH - H \frac{\cos\varphi_0}{\cos\varphi} \frac{\partial}{\partial x'} \left[\frac{p_s}{\rho_0} + g(\zeta - \eta) \right]$$
$$\left. - (\tau_* - \tau_0) UH + \frac{\tau_{s\lambda}}{\rho_0} \right\} + \frac{\partial}{\partial y'} \left\{ V \frac{\partial \zeta}{\partial t} - \frac{\cos\varphi_0}{\cos\varphi} UH \frac{\partial V}{\partial x'} \right. \tag{10}$$
$$- VH \frac{\partial V}{\partial y'} - \left(\frac{\tan\varphi}{R} U + f \right) UH - H \frac{\partial}{\partial y'} \left[\frac{p_s}{\rho_0} + g(\zeta - \eta) \right]$$
$$\left. - (\tau_* - \tau_0) VH + \frac{\tau_{s\varphi}}{\rho_0} \right\} + \frac{\partial}{\partial t} \left(\frac{\tan\varphi}{R} VH \right) - \tau_0 \left(\frac{\tan\varphi}{R} VH \right) = 0$$

The GWCE (Equation 10) is solved in conjunction with the primitive momentum equations in nonconservative form (Equations 8 and 9).

The high accuracy of GWCE-based FE solutions is a result of their excellent numerical amplitude and phase propagation characteristics. In fact Fourier analysis indicates that in constant depth water and using linear interpolation, a linear tidal wave resolved with 25 nodes per wavelength is more than adequately resolved over the range of Courant numbers: $C = \sqrt{gh}\,\Delta t/\Delta x \leq 1.0$ (Luettich, Westerink, and Scheffner 1992). Furthermore, the monotonic dispersion behavior of GWCE-based FE solutions avoids generating artificial near $2 \cdot \Delta x$ modes, which plague primitive-based FE solutions (Platzman 1981, Foreman 1983). The monotonic dispersion behavior of GWCE-based FE solutions is very similar to that associated with staggered finite difference solutions to the primitive shallow-water equations (Westerink and Gray 1991). GWCE-based FE solutions to the shallow-water equations permit extremely flexible spatial discretizations, which can substantially reduce the discrete size of any problem (Le Provost and Vincent 1986, Foreman 1988, Vincent and Le Provost 1988, Westerink et al. 1992).

The details of ADCIRC and the implementation of the GWCE-based solution to the shallow-water equations are described by Luettich, Westerink, and Scheffner (1992). As with most GWCE-based FE codes, ADCIRC applies three-noded linear triangles for surface elevation, velocity, and depth. Furthermore, the decoupling of the time-independent and/or tridiagonal system matrices, elimination of spatial integration procedures during time-stepping, and full vectorization of all major loops result in a highly efficient code.

3 Description of the Computational Domain

The ENPACT model domain, shown in Figure 1, includes most of the eastern North Pacific, the Gulf of California, and the Guatemala and Panama Basins. The curved open boundary stretches from Seal Cape on Unimak Island, Alaska, in the north, to Punta Parada, Peru, in the south. The land boundary includes the Pacific coastlines of Alaska, Canada, mainland U. S., Mexico, Guatemala, El Salvador, Nicaragua, Costa Rica, Panama, Columbia, and Northern Peru.

Although the focus of this model is on the U.S. west coast and Alaska, the larger scale physics of the eastern Pacific must also be considered. A number of diurnal and semidiurnal amphidromes exist in the deep ocean which have a substantial effect on the tides in the coastal areas. Cartwright, Ray, and Sanchez (1991) established the approximate locations of these amphidromes using Geosat altimetry. Figure 1 shows the approximate locations of these amphidromes. Due west of southern California are M_2, S_2, and N_2 amphidromes; west of the Galapagos Islands amphidromes exist for the K_1, O_1, M_2, S_2, and N_2 constituents. Since spatial variations in phase are rapid near amphidromes, it would be extremely difficult to specify accurate open boundary conditions near any of these features. For this reason, the ENPACT model's open boundary is located well away from all of these amphidromes. In addition, the vast southern extent of the domain allows inclusion of large-scale effects on the U.S. west coast tides arising from the complex tides in the Panama Basin and the Gulf of California. However, the open boundary is not so far offshore that the presence of additional observed M_2, S_2, and N_2 amphidromes to the south, and the Hawaiian Islands to the west, would introduce additional complications.

Further, the model open boundary is almost entirely in the deep ocean, well away from the continental shelf and slope where nonlinear constituents are important but difficult to determine. (Where the open ocean boundary meets the land in the Aleutian Peninsula and in Peru, the continental shelf and slope are very narrow so the effects of nonlinear tides in these areas should be negligible.) This positioning simplifies the specification of open boundary conditions considerably. It also facilitates the coupling of the ENPACT model with global tidal models which are most accurate in the deep ocean. Finally, the

geometrically simple open boundary follows a single smooth continuous arc, avoiding the complications which arise when multiple boundaries and boundaries with sharp corners are used.

Land boundaries in the ENPACT model were derived from the World Data Bank II geophysical database (NGDC 1993). This database provides an accurate digital representation of all major coastline features and islands and is particularly well-suited for large scale models.

Model bathymetry is shown in Figure 2. Depths range from over 6,000 m in the Aleutian Trench to less than 1 m near shore. The continental shelf is very narrow in most areas, and extremely sharp bathymetric gradients exist along the continental shelf and slope. All bathymetric data for the model were obtained from the ETOPO-5 database (NGDC 1988), which has a 5-min by 5-min resolution. Depths at each grid node were linearly interpolated from this database.

By taking advantage of the grid flexibility permitted by the finite element method, grid points in the model are concentrated in areas with rapidly varying bathymetry and/or complex shoreline geometry. Conversely, fewer grid points are used in the open ocean and the deep Guatemala Basin (Figure 3). The triangular finite element grid was generated using ACE/gredit, a flexible, interactive, graphical software package (Turner and Baptista 1991). In areas of the grid where depths exceed 3,000 m, resolution is about 0.5 deg (about 44 km). Between the 1,000-m and 3,000-m isobaths, grid resolution is about 15 min (about 22 km). North of Cabo Corrientes, Mexico, and above the 1,000-m isobath, grid resolution is 7.5 min (about 11 km). In some nearshore areas such as Cook Inlet, Alaska, and Puget Sound, Washington, the grid resolution is even finer. Transitions from larger elements to smaller elements are smooth, and all elements in the grid passed a stringent screening for skewness.

Extensive grid convergence studies conducted with a large-scale model of the western North Atlantic (Westerink, Luettich, and Muccino 1994; Luettich and Westerink, in press) suggest that the ENPACT grid should be adequate to resolve most flow features of interest. In addition, since grid resolution in nearshore areas is roughly at the same resolution as the ETOPO-5 database, further grid refinement in these areas would be of limited benefit without additional bathymetric data.

The final grid used for the tidal simulations has 27,494 nodes. This is about one-fourth of the approximately 100,000 nodes which would be required if the domain were discretized at a uniform resolution of 7.5 min.

4 Tidal Simulations with the ENPACT Model

The tidal simulations were performed using the hydrodynamic code ADCIRC-2DDI (version 25.05). The runs included the finite amplitude and convective acceleration terms, as well as nonlinear bottom friction. In addition, spatially varying Coriolis and tidal potential terms were included, both of which are essential when modeling a domain of this size. The bottom friction coefficient was set equal to 0.003 (Chow 1959) for the entire domain. Since the runs were intended to be entirely predictive, no attempt was made to tune this parameter.

Details of the model input requirements and the use of its preprocessor, ADCSETUP, are given in Westerink et al. (1994). Key model parameters for the ENPACT model runs are summarized briefly next. Using a time-step of 37.5 sec, the minimum and maximum wave celerity-based Courant numbers ($C = \sqrt{gh}\,\Delta t/\Delta x$) in the grid were 0.01 and 0.99, respectively. To avoid drying of computational elements, a minimum depth of 6 m was set for the entire domain. Time weighting factors of 0.35, 0.30, and 0.35 were used for the future, current, and past time levels of the GWCE. The weighting coefficient for the primitive portion of the GWCE, τ_0, was set to 0.001. Center point longitude and latitude for the CP projection were: λ_0 = 125° W, and φ_0 = 21° N.

The open boundary was forced with two diurnal astronomical constituents, K_1 and O_1; and with three semidiurnal astronomical constituents, M_2, S_2, and N_2. These boundary conditions were obtained by interpolating results from a finite element global ocean model (Le Provost et al. 1994) onto each of the model's open boundary nodes. In the deep ocean these boundary conditions show good agreement with the observed values of Cartwright, Ray, and Sanchez (1991) and the International Hydrographic Organization (IHO) (1990). In addition, they appear to be an improvement over the widely used Schwiderski (1980) global model, which was shown to overpredict many of the constituents in a detailed study of the western North Atlantic (Westerink, Luettich, and Muccino 1994). The range of values used to force the open boundary is presented in Table 2. Tidal potential forcing was applied using the same constituents as were used at the open boundary. The tidal potential

constants and the constituent-dependent earth elasticity factors are given in Table 3.

The model was spun up from rest using a smooth hyperbolic tangent ramp, acting on both the open boundary and direct forcings for 15 days. The use of this ramp sharply reduces the generation of short-period gravity and vortex modes due to startup transients. The model simulation was a total of 62 days long, the first 30 days of which were discarded to ensure that any lingering startup transients had dissipated. A least-squares harmonic analysis was performed on the remaining 32 days.

To confirm that the model had reached a state of dynamic equilibrium, the model was run for an additional 33 days (to day 95) and a separate, independent harmonic analysis conducted. Figure 4 shows the amplitude and phase differences between the harmonic analysis done for days 30 through 62 and the harmonic analysis for days 63 through 95, for the M_2 and K_1 constituents. Amplitude differences for the M_2 tide are typically less than 0.1 cm, and nowhere in the domain are they greater than 0.5 cm. Phase differences for the M_2 tide are typically less than 1 deg for the entire domain, and nowhere are the differences greater than 2 deg -- even near amphidromes. The K_1 tide shows similar behavior, although the magnitudes of the differences are slightly higher. K_1 amplitude differences are typically 1 cm, and phase differences are typically less than 1 deg. In Puget Sound, WA, which is poorly resolved in this grid, K_1 amplitude differences approach 5 cm and phase differences approach 9 deg. However, for the vast majority of the domain, there are no meaningful differences between the two analyses. Therefore, the results of this comparison indicate that the model had indeed reached dynamic steady-state by the end of the initial 32 days. It also demonstrates the ability of the ADCIRC code to run for over 3 months without generation of spurious modes.

The computational efficiency of the model was very good. A number of techniques have been implemented in ADCIRC to improve model performance including full vectorization of all major loops and the use of time-independent and/or tridiagonal system matrices. In addition, ADCIRC has the capability to use a variety of iterative compact storage solvers from the ITPACKV 2D package (Kincaid, Oppe, and Young 1989). These iterative solvers have excellent stability and accuracy characteristics and are much more memory-efficient than conventional banded matrix solvers, especially for large problems. For the 27,494-node ENPACT grid, the total CPU time on a Cray Y-MP 8/8128 for the 62-day simulation including a 20-frequency harmonic analysis was 19.79 hr. On the same machine, the maximum memory required for the simulation was 5.87 MWords.

5 Comparison Between Computed and Observed Tidal Elevations in the ENPACT Model

The coupled global/ENPACT model results allow for realistic comparisons with observed tidal elevation data. A relatively large number of these data are available for the coastal areas of the eastern Pacific in harmonically decomposed form from the International Hydrographic Organization Tidal Constituent Bank (1990). Only observational data with record durations longer than 189 days were used to ensure reliability and consistency. However, for some places in the domain long tidal records were unavailable. In these areas (typically at offshore locations), short-term observational data were used to improve the spatial coverage of the comparisons. Table 1 presents the station locations and record durations for each observational station. Figure 5 shows the position of each station within the model domain.

Model physics include the full set of nonlinear terms in the shallow-water equations and therefore allow constituents to interact with themselves and each other to generate overtides and compound tides. Results from the simulations were harmonically analyzed using half-hour sampling from the final 32 days of the simulation. Employing a least-squares method, results were decomposed into 20 frequencies. Although only the five astronomical forcing frequencies with observed data were compared, fourteen additional overtide and compound frequencies and a steady component were included in the harmonic analysis to more accurately separate individual constituents from the tidal signal. The computations were intended to be entirely predictive, so no calibration or tuning procedures were performed to improve agreement between model results and observed values.

Cotidal charts for the two diurnal constituents and the three semidiurnal constituents are presented in Figures 6 and 7. The diurnal constituents show a strong similarity to each other. Diurnal amplitudes show a steady increase with latitude up into the Gulf of Alaska. The K_1 and O_1 tides each have amphidromes west of the Galapagos Islands. Much of the U.S. coast is nearly in phase for the diurnal tides. The semidiurnals also show a strong similarity

to each other. Semidiurnal amplitudes markedly increase as these tides propagate into the Gulf of Alaska and into the Guatemala and Panama basins. Extremely sharp increases in amplitude occur in Cook Inlet, AK, and along the Canadian coast where the continental shelf is relatively wide. The M_2, S_2, and N_2 phases each exhibit twin amphidromes in the deep ocean. Large stretches of the U.S. west coast are within 60 deg of being in phase for these constituents.

The accuracy of the tidal simulations was quantified by comparing modeled values at the 72 stations with observed values on a constituent-by-constituent basis. Figures 6 and 7 shows relative amplitude errors and absolute phase errors at each of the 72 stations. To more readily identify trends in the comparisons, the stations were grouped into five separate regions. The station groupings are as follows: South and Central America (stations 1-19), U.S. west coast (stations 20-41), Canada and Alaska (42-64), and Offshore (stations 65-72). For each of the defined regions as well as for the entire domain, the amplitude error for constituent j for each of the five astronomical constituents was computed as a proportional standard deviation:

$$E_{j\text{-}amp}^{calc\text{-}obs} = \left\{ \frac{\sum_{l=1}^{L} \left[\hat{\eta}_j^{calc}(x_l,y_l) - \hat{\eta}_j^{obs}(x_l,y_l) \right]^2}{\sum_{l=1}^{L} \left[\hat{\eta}_j^{obs}(x_l,y_l) \right]^2} \right\}^{1/2} \tag{11}$$

where

L = total number of elevation stations within a given region

(x_l,y_l) = location of an elevation station

$\hat{\eta}_j^{calc}(x_l,y_l)$ = computed elevation amplitude for constituent j at station coordinates (x_l,y_l)

$\hat{\eta}_j^{obs}(x_l,y_l)$ = observed elevation amplitude for constituent j at station coordinates (x_l,y_l)

The phase error for each constituent j was computed as an absolute average error defined over a region as:

$$E_{j\text{-}phase}^{calc\text{-}obs} = \frac{1}{L} \sum_{l=1}^{L} \left| \varphi_j^{calc}(x_l,y_l) - \varphi_j^{obs}(x_l,y_l) \right| \tag{12}$$

where

$\varphi_j^{calc}(x_l,y_l)$ = computed elevation phase for constituent j at station coordinates (x_l,y_l)

$\varphi_j^{obs}(x_l,y_l)$ = observed elevation phase for constituent j at station coordinates (x_l,y_l)

Amplitude and phase errors are presented in Tables 4 and 5 for the entire domain as well as on a regional basis for each of the five astronomical constituents. For all 72 stations in the domain all constituents are predicted with an average amplitude error between 15.3 and 65.5 percent and an average phase error between 5.0 and 66.2 deg. In general, the amplitude errors are smaller at the offshore and South and Central America stations where the tides are relatively small. Along the U.S. west coast amplitude errors are relatively large, particularly for the S_2 constituent. Phase errors show no predominant trends in spatial variability.

The distribution of amplitude ratio errors for each constituent is presented in Table 6. In general the predicted values for the diurnal constituents are closely grouped around the observed values, with a slight bias toward overprediction. The semidiurnal constituents show quite dissimilar behavior among themselves. The M_2 constituent shows a somewhat uniform distribution around the observed values with a small peak at the mean. The S_2 constituent is in general grossly over-predicted, but with a large number of under-predicted outliers as well. Finally, the calculated values for the N_2 constituent tightly grouped around the observed values with relatively few outliers.

Table 7 gives the distribution of phase error for each constituent. Phase predictions for the two diurnal constituents, K_1 and O_1, are quite good with most stations within ± 10 deg of the observed values. The M_2 and particularly the S_2 tide tend to lead the observations by a large margin. Finally, the calculated N_2 shows a wide distribution of phase error with the highest percent of stations being ahead of the observed phase.

Resynthesized surface elevation time histories derived from both the computed and observed constituent data are shown for representative stations in Figure 8. Computed time histories were resynthesized from harmonically decomposed ENPACT model results for the five astronomical forcing constituents. Observed time histories were resynthesized in the same manner. Appendix A provides procedures for resynthesis.

These time histories show the types of tides which occur in the eastern North Pacific and are useful for making general comparisons between model results and the observed tides. Along South and Central America, the tides are mixed semidiurnal. The tides become decreasingly mixed with increasing latitude, and north of Washington state they are almost completely semidiurnal.

6 Discussion

The ability of a numerical model to successfully simulate environmental scale flows depends on the physics included in the model, the numerical accuracy (which depends on the algorithm as well as the grid), the representation of the bathymetry and the land geometry, and the precision of the forcing functions. Two-dimensional barotropic models generally give comparisons between model predictions and measurements within 10-percent accuracy for amplitude and 10-percent accuracy for phase. Therefore, it is assumed that the physics incorporated into ADCIRC-2DDI should be generally satisfactory for large-scale tidal simulations. However, it should be noted that in localized coastal areas where the water column is strongly stratified or where freshwater inflows are large, the model physics may be not be adequate.

The high numerical accuracy of GWCE-based finite element models, including ADCIRC-2DDI, is well documented (e.g., Lynch and Gray 1979; Le Provost and Vincent 1986; Luettich, Westerink, and Scheffner 1992). Grid properties of the model are quite good: all elements are close to equilateral in shape, adjacent elements are of similar sizes, and nodal support is even throughout the domain. Earlier grid convergence studies (Westerink, Luettich, and Muccino 1994; Luettich and Westerink, in press) indicate that the ENPACT model grid should be reasonably converged for most areas within the domain for the K_1, O_1, M_2, S_2, and N_2 tides.

Inaccurate representation of the bottom topography in the model is likely to be a major source of error in the results, particularly near the coast. In deep water, Smith (1993) found that the ETOPO-5 database could have a mean error of 26 m. In nearshore areas, where bathymetric gradients are the largest, ETOPO-5 bathymetric data are the least accurate. Further, although the ETOPO-5 database has a uniform resolution of 5 min by 5 min, the original data from which it was derived have a highly variable spatial density. Above the 200-m isobath, ETOPO-5 soundings are the most sparse and least reliable.[1] One improvement that could be made to the present study would be to use more accurate representations of the bottom with higher resolution digital bathymetric data as they become available.

[1] Personal Communication, June 1994, P.W. Sloss, NOAA-NGDC, Boulder, CO.

The open boundary conditions which were interpolated from a global ocean model (Le Provost et al., in press) are spatially smooth and in general show good agreement with the observational data of Cartwright, Ray, and Sanchez (1991) and the IHO (1990). However, the coupled global/ENPACT model results show large differences from observed values in the deep ocean. Offshore the forced constituent tides are quite complex due to the presence of multiple amphidromes. Horizontal translations in the position of any of these amphidromes can have a basin scale effect on the tides (Luettich and Westerink, in press), although the areas closest to the amphidromes will usually show the largest relative change.

Comparisons with observed results suggest that several localized areas of the grid require additional resolution. For example, on the Washington shelf and at the mouth of the Strait of Juan de Fuca model, results are reasonably accurate. However, in the immediately adjacent waters of Puget Sound, model predictions are much less accurate. Similar behavior is seen in Prince William Sound, AK. These areas are ideal candidates for regional-scale high-resolution models which could provide a more precise representation of the bathymetry and coastal geometry and be forced with the results from the coupled global/ ENPACT model.

The results obtained from this study are generally less accurate than those obtained from a similar modeling effort along the U.S. east coast, the Gulf of Mexico, and the Caribbean Sea (Westerink, Luettich, and Scheffner 1993). While it is not entirely clear why this should be, the most likely explanations would seem to be inaccurate bathymetry and poor offshore boundary conditions. It is also possible that the model needs to be run with a radiative boundary condition to allow energy to propagate out of the domain. This may be particularly important for the eastern North Pacific, which has much steeper (and hence more reflective) bottom topography and much narrower (and hence less dissipative) shelves than along the U.S. east coast.

7 Conclusions

The ENPACT model is a large-domain coastal ocean model with a geometrically and hydrodynamically simple open boundary. The large domain simplifies open boundary specification and allows inclusion of large-scale effects arising from the Gulf of California and the Guatemala and Panama Basins. The inclusion of these large-scale effects adds little to the size of the discrete problem since the model uses a variable-spaced grid.

The model was forced with five astronomical constituents on the open boundary derived from a state-of-the-art global tidal model. In addition, a realistic tidal potential forcing was applied to the interior of the domain. The simulations were intended to be entirely predictive, so no tuning or calibration procedures were performed.

Comparison between model results and field data was made at 72 stations distributed throughout the domain for the K_1, O_1, M_2, S_2, and N_2 constituents. Average amplitude errors for all the stations range from 15.3 to 65.5 percent, and average errors in phase range from 5.0 to 66.2 deg. Some modeled constituents (e.g., O_1) show excellent agreement with observations, while others (e.g., S_2) are poorly predicted. Phase errors along the coast are quite sensitive to the position of offshore amphidromes. Even in the deep ocean, there is no close match between predictions and observations. Potential reasons for these discrepancies include inaccurate bathymetry, poor elevation open boundary conditions, and the lack of a radiative condition along the model open boundary.

References

Cartwright, D. E., Ray, R. D., and Sanchez, B. V. (1991). "Oceanic tide maps and spherical harmonic coefficients from geosat altimetry," NASA Tech. Memo. 104544, Goddard Space Flight Center, Greenbelt, MD.

Chow, V. T. (1959). *Open channel hydraulics*. McGraw-Hill, New York.

Flather, R. A. (1987). "A tidal model of the northeast Pacific," *Atmosphere-Ocean* 25(1), 22-45.

_____. (1988). "A numerical model investigation of tides and diurnal-period continental shelf waves along Vancouver Island," *J. of Physical Oceanography* 18, 115-139.

Foreman, M. G. G. (1977). "Estimates of extreme conditions of tide and surge using a numerical model of the North-west European continental shelf," *Estuarine, Coastal and Shelf Science* 24, 69-73.

_____. (1983). "An analysis of the wave equation model for finite element tidal comparisons," *Journal of Computational Physics* 52, 290-312.

_____. (1988). "A comparison of tidal models for the southwest coast of Vancouver Island." *Proceedings of the VII International Conference on Computational Methods in Water Resources*, Cambridge, MA. Elsevier Science Publishing Co., New York.

Foreman, M. G. G., Henry, R. F., Walters, R. A., and Ballantyne, V. A. (1993). "A finite element model for the tides and resonance along the north coast of British Columbia," *Journal of Geophysical Research* 98 (C2), 2509-2531.

Gray, W. G. (1982). "Some inadequacies of finite element models as simulators of two-dimensional circulation," *Advances in Water Resources* 5, 171-177.

Hendershott, M. C. (1981). "Long waves and ocean tides," *Evolution of physical oceanography*, B. A. Warren and C. Wunsch, eds., MIT Press, Cambridge, MA, 292-341.

International Hydrographic Organization. (1990). *Tidal constituent bank, station catalogue*, Ocean and Aquatic Sciences, Department of Fisheries and Oceans, Ottawa, Canada.

Kincaid, D. R., Oppe, T. C., and Young, D. M. (1989). "ITPACKV 2D users guide," Report CNA-232, Center for Numerical Analysis, The University of Texas at Austin.

Kinnmark, I. P. E. (1984). "The shallow water wave equations: Formulation, analysis and application," Ph.D. dissertation, Department of Civil Engineering, Princeton University, NJ.

Kolar, R. L., Gray, W. G., Westerink, J. J., and Luettich, R. A., Jr. (1994). "Shallow water modeling in spherical coordinates: Equation formulation, numerical implementation, and application," *Journal of Hydraulic Research* 32 (1), 3-24.

Leenknecht, D. A., Szuwalski, A., and Sherlock, A. R. (1992). "Automated coastal engineering system - technical reference," Technical Note No. CETN-VI-20, U.S. Army Engineer Waterways Experiment Station, Vicksburg, MS.

Le Provost, C., and Vincent, P. (1986). "Some tests of precision for a finite element model of ocean tides," *Journal of Computational Physics* 65, 273-291.

Le Provost, C., Genco, M. L., Lyard, F., Vincent, P., and Canceill, P. (1994). "Spectroscopy of the world ocean tides from a hydrodynamic finite element model," *Journal of Geophysical Research* 99(C12):24,777-24,797.

Luettich, R. A., Jr., and Westerink, J. J. "Continental shelf scale convergence studies with a barotropic tidal model." *Quantitative skill assessment for coastal ocean models.* D. R. Lynch and A. M. Davies, eds., AGU Press, Washington, DC, in press.

Luettich, R. A., Jr., Westerink, J. J., and Scheffner, N. W. (1992). "ADCIRC: An advanced three-dimensional circulation model for shelves, coasts, and estuaries; Report 1, Theory and methodology of ADCIRC-2DDI and ADCIRC-3DL," Technical Report DRP-92-6, U.S. Army Engineer Waterways Experiment Station, Vicksburg, MS.

Lynch, D. R., and Gray, W. G. (1979). "A wave equation model for finite element tidal computation," *Computers and Fluids* 7, 207-228.

National Geophysical Data Center. (1988). "ETOPO-5 bathymetry/topography data," *Data Announc. 88-MGG-02*, Natl. Oceanic and Atmos. Admin., U.S. Dept. Commerce, Boulder, CO.

Lynch, D. R., and Gray, W. G. (1993). "Global relief CD-ROM data," *Data Announc. 93-MGG-01*, Natl. Oceanic and Atmos. Admin., U. S. Dept. Commerce, Boulder, CO.

Pearson, F. (1990). *Map projections: Theory and applications*. CRC Press, Inc., Boca Raton, FL.

Platzman, G. W. (1981). "Some response characteristics of finite element tidal models," *Journal of Computational Physics* 40, 36-63.

Reid, R. O. (1990). "Waterlevel changes." *Handbook of coastal and ocean engineering*, J. Herbich, ed., Gulf Publishing, Houston, TX.

Schureman, P. (1941). *Manual of harmonic analysis and prediction of tides*. Special Publication No. 98, Coast and Geodetic Survey, U.S. Department of Commerce, U.S. Government Printing Office, Washington, DC.

Schwiderski, E. W. (1980). "On charting global ocean tides," *Reviews in Geophysics and Space Physics* 18, 243-268.

Smith, W. H. F. (1993). "On the accuracy of digital bathymetric data," *Journal of Geophysical Research* 98(B6), 9591-9603.

Turner, P. J., and Baptista, A. M. (1991). "ACE/gredit users manual: Software for semi-automatic generation of two-dimensional finite element grids," CCALMR Software Report SDS2 (91-2), Oregon Graduate Institute, Beaverton, OR.

Vincent, P., and Le Provost, C. (1988). "Semidiurnal tides in the Northeast Atlantic from a finite element numerical model," *Journal of Geophysical Research* 93(C1), 543-555.

Wahr, J. M. (1981). "Body tides on an elliptical, rotating, elastic and oceanless earth," *Geophys. J. R. Astr. Soc.* 64, 677-703.

Westerink, J. J., and Gray, W. G. (1991). "Progress in surface water modeling," *Reviews of Geophysics*, April supplement, 210-217.

Westerink, J. J., Blain, C. A., Luettich, R. A., Jr., and Scheffner, N. W. (1994). "ADCIRC: An advanced three-dimensional circulation model for shelves, coasts and estuaries; Report 2, User's manual for ADCIRC-2DDI," Technical Report DRP-92-6, U.S. Army Engineer Waterways Experiment Station, Vicksburg, MS.

Westerink, J. J., Luettich, R. A., Jr., and Muccino, J. C. (1994). "Modeling tides in the Western North Atlantic using unstructured graded grids," *Tellus* 46(A), 178-199.

Westerink, J. J., Luettich, R. A., Jr., and Scheffner, N. (1993). "ADCIRC: An advanced three-dimensional circulation model for shelves, coasts and estuaries; Report 3, Development of a tidal constituent database for the western North Atlantic and Gulf of Mexico," Technical Report DRP-92-6, U.S. Army Engineer Waterways Experiment Station, Vicksburg, MS.

Westerink, J. J., Luettich, R. A., Jr., Baptista, A. M., Scheffner, N. W., and Farrar, P. (1992). "Tide and storm surge predictions using a finite element model," *Journal of Hydraulic Engineering* 118, 1373-1390.

Woodworth, P. L. (1990). "Summary of recommendations to the UK Earth Observation Data Centre (UK-EODC) by the Proudman Oceanographic Laboratory (POL) for tide model corrections on ERS-1 geophysical data records," Proudman Oceanographic Laboratory Communication, Bidston, UK.

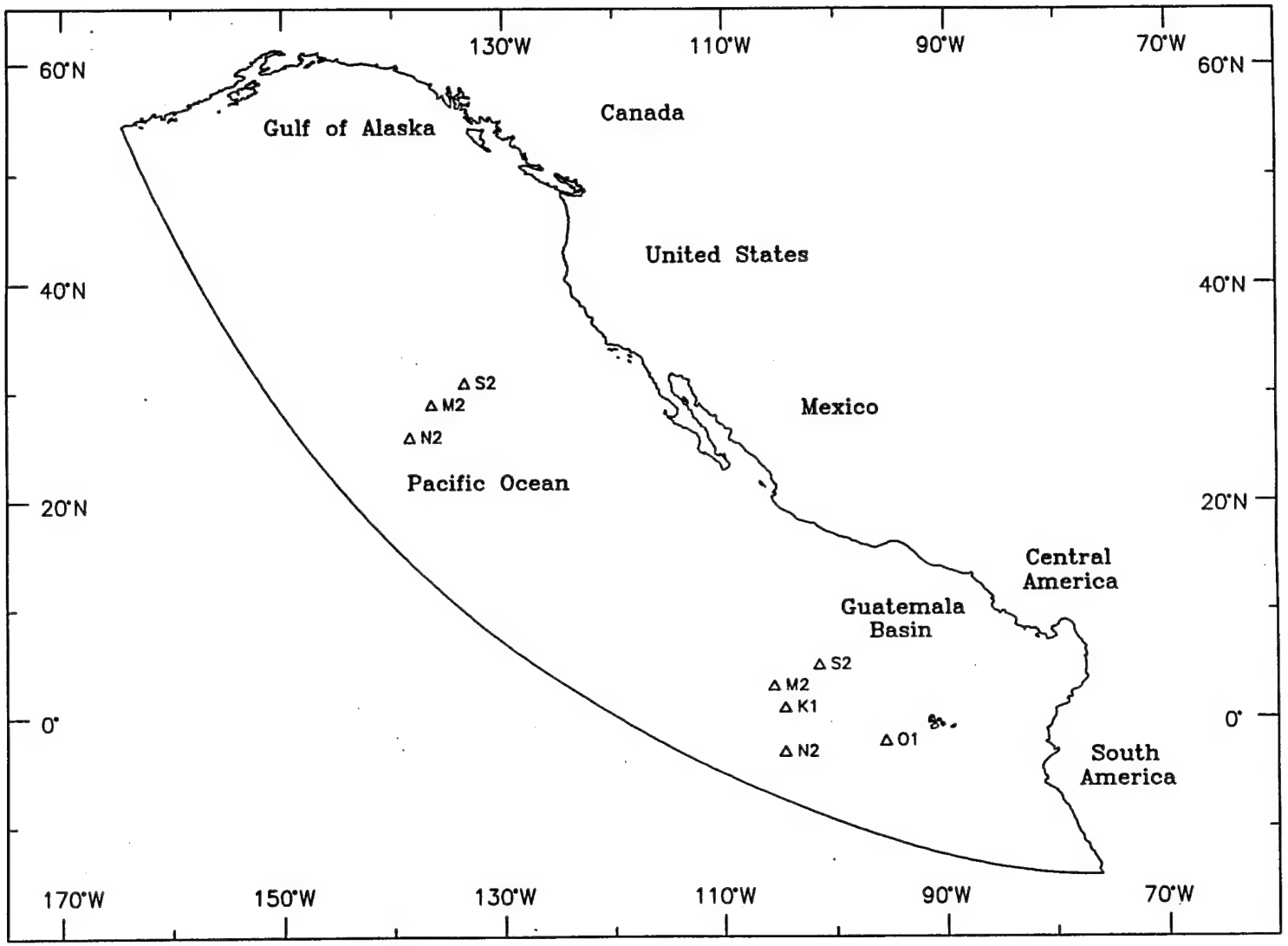

Figure 1. The Eastern North Pacific Tidal (ENPACT) model computational domain; approximate locations of known amphidromes determined from Geosat altimetry (Cartwright, Ray, and Sanchez 1991) are denoted by a triangle and the constituent

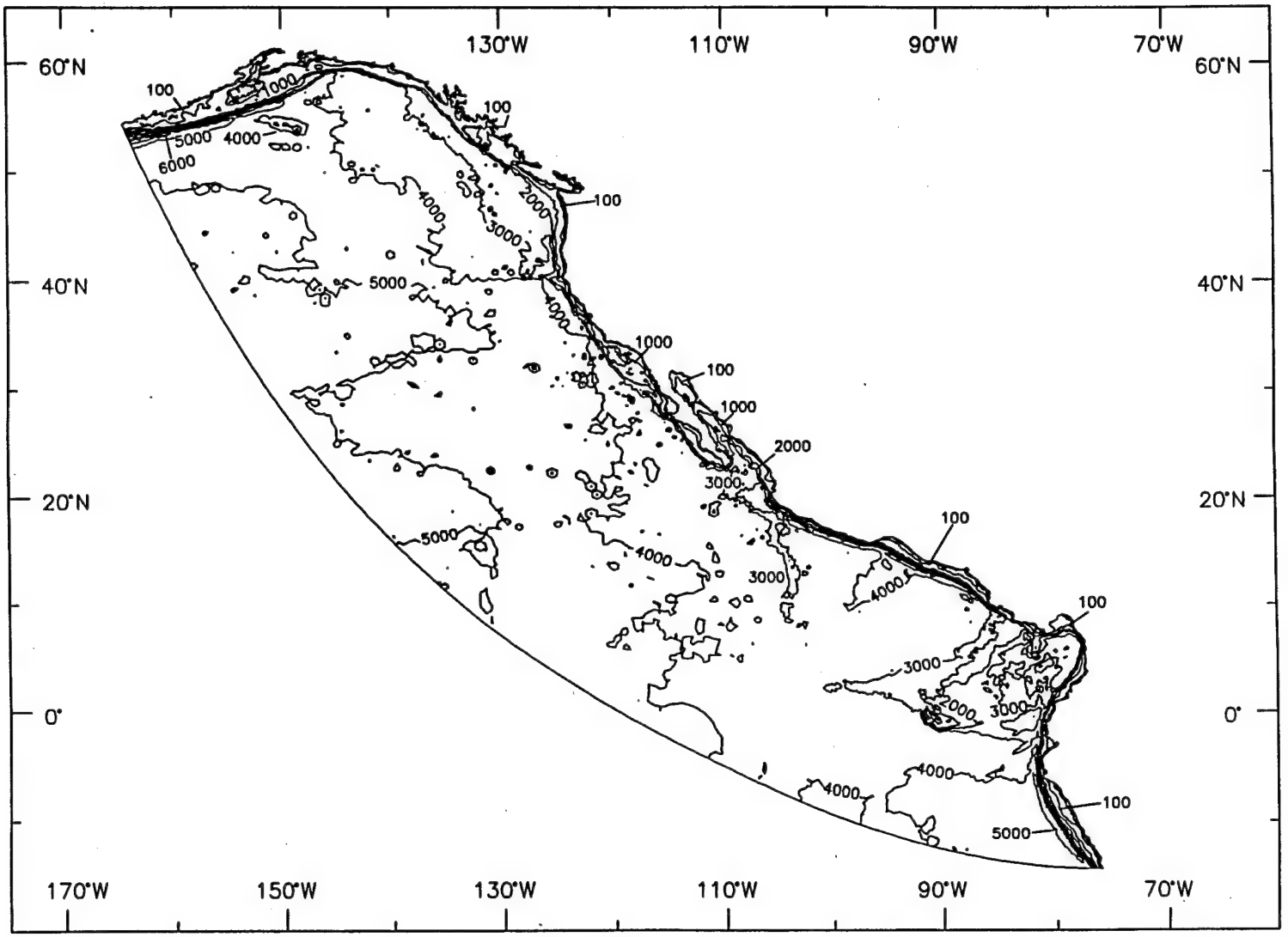

Figure 2. Bathymetry contours (meters) within the ENPACT model domain

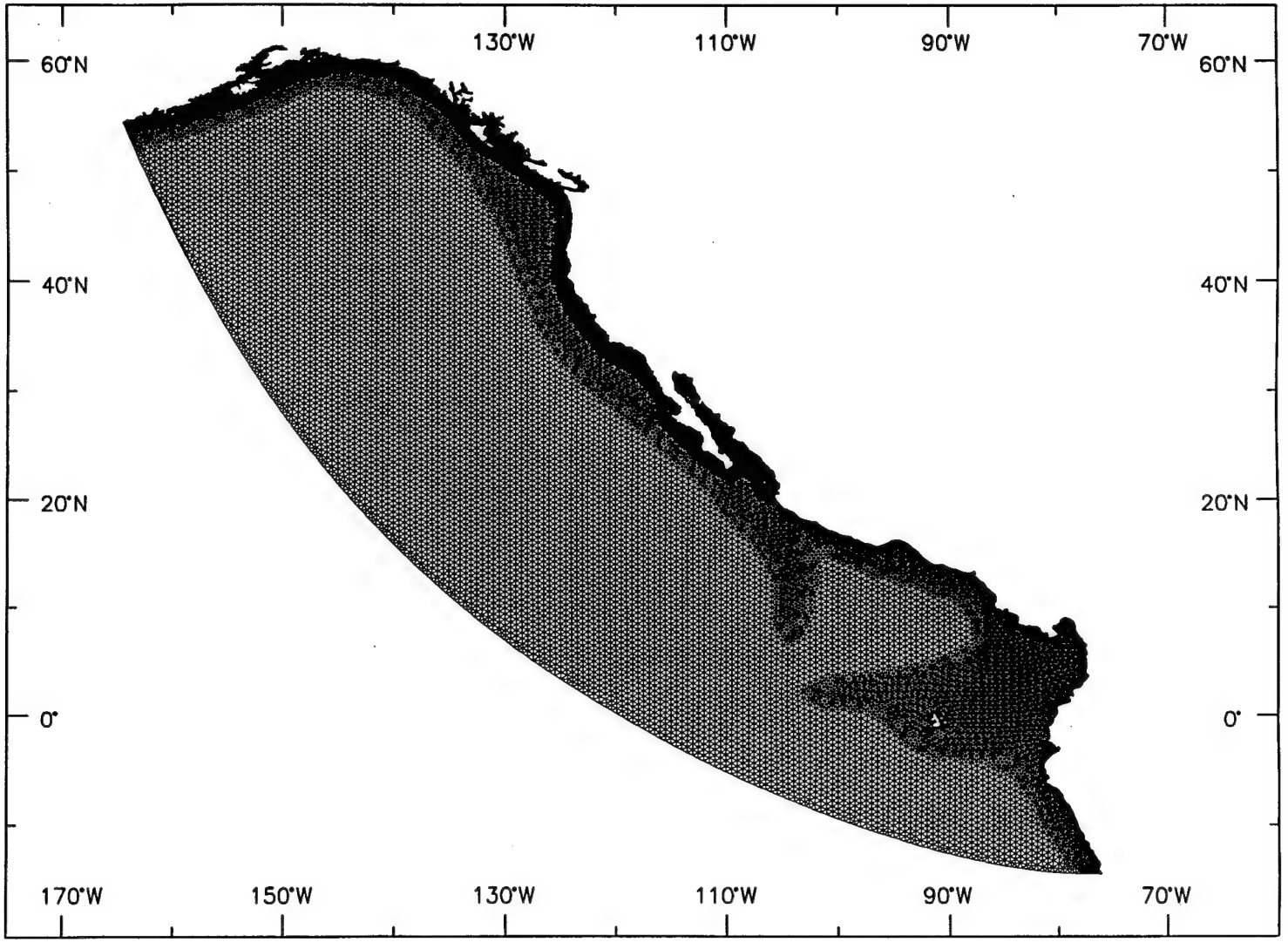

Figure 3. Graded finite element grid with resolution ranging from 0.5 deg to less than 7.5 min

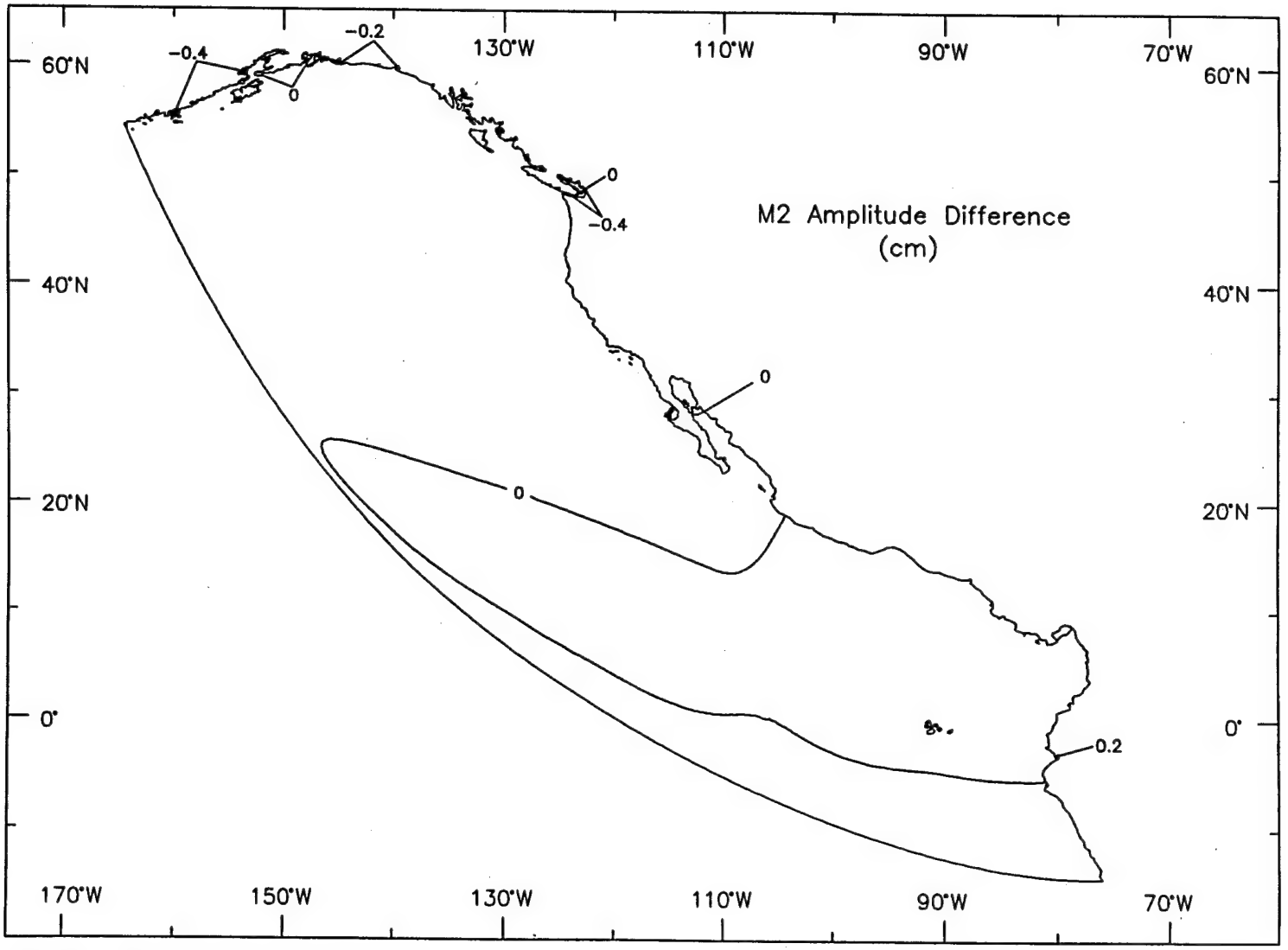

Figure 4. Computed contours showing absolute differences between harmonic analysis done for days 30 through 62 and harmonic analysis done for days 63 through 95. M2 amplitude and phase contour intervals are 0.1 cm and 0.5 deg, respectively. K1 amplitude and phase contour intervals are 1.0 cm and 1.0 deg, respectively (Sheet 1 of 4)

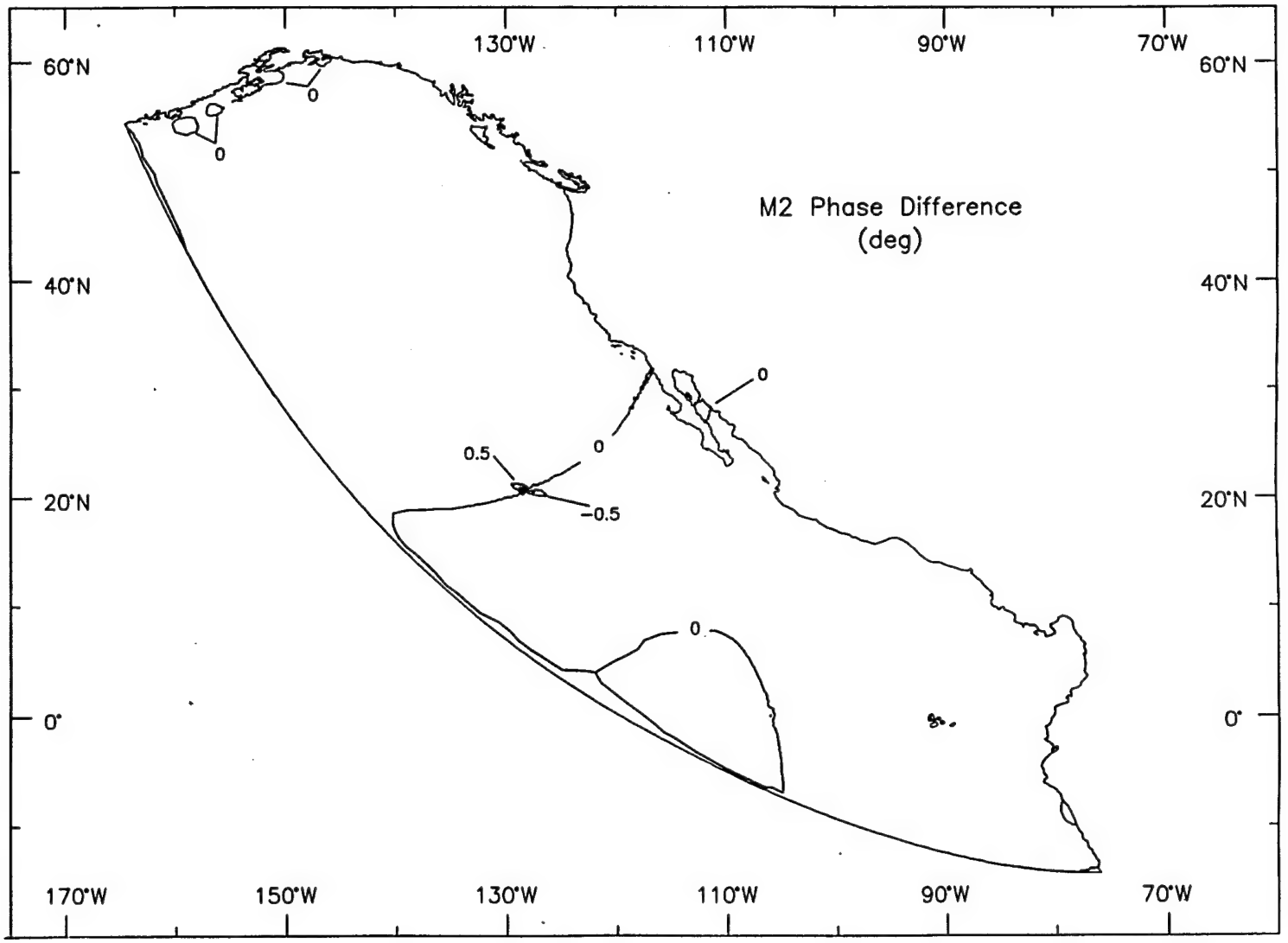

Figure 4. (Sheet 2 of 4)

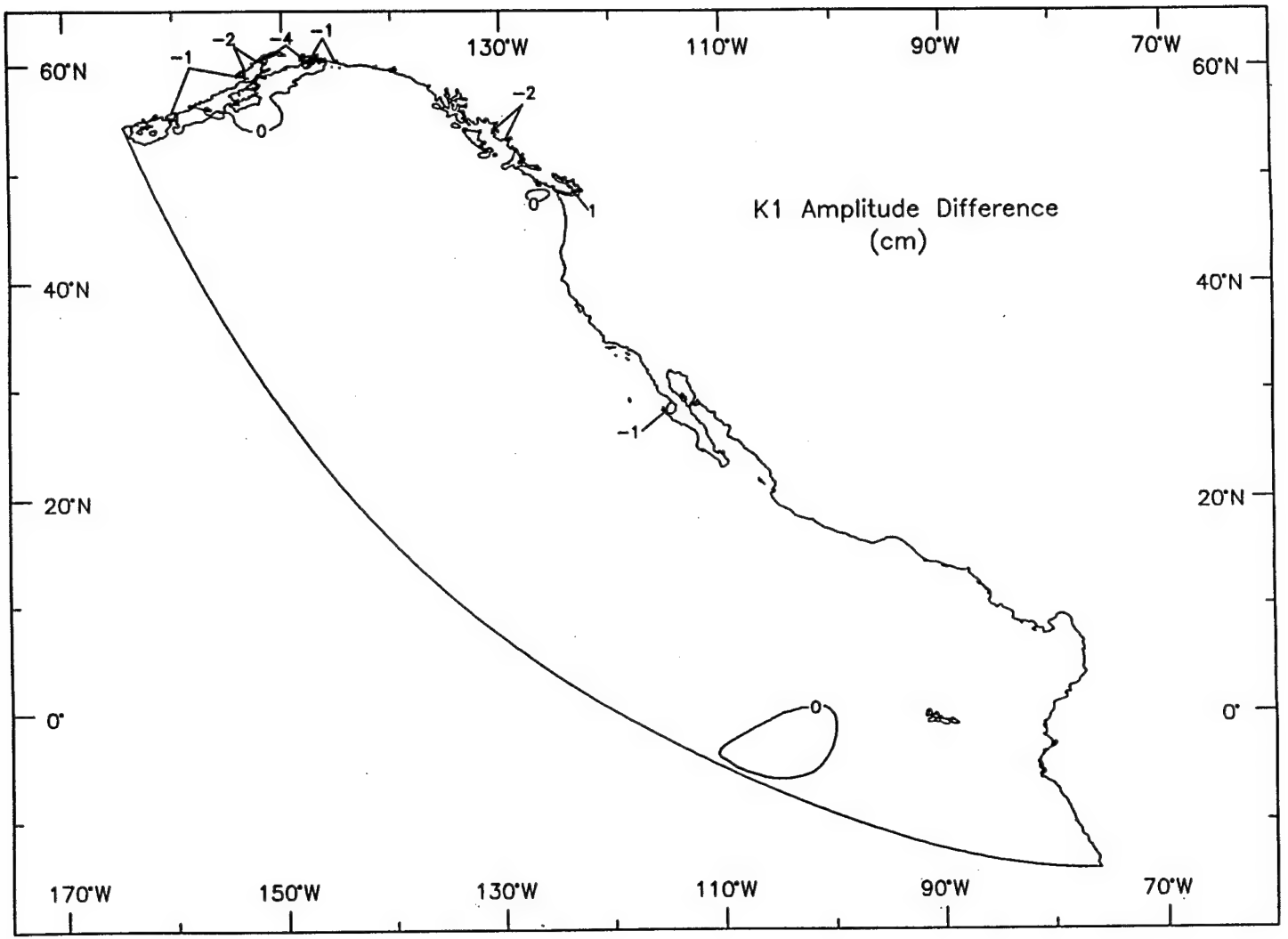

Figure 4. (Sheet 3 of 4)

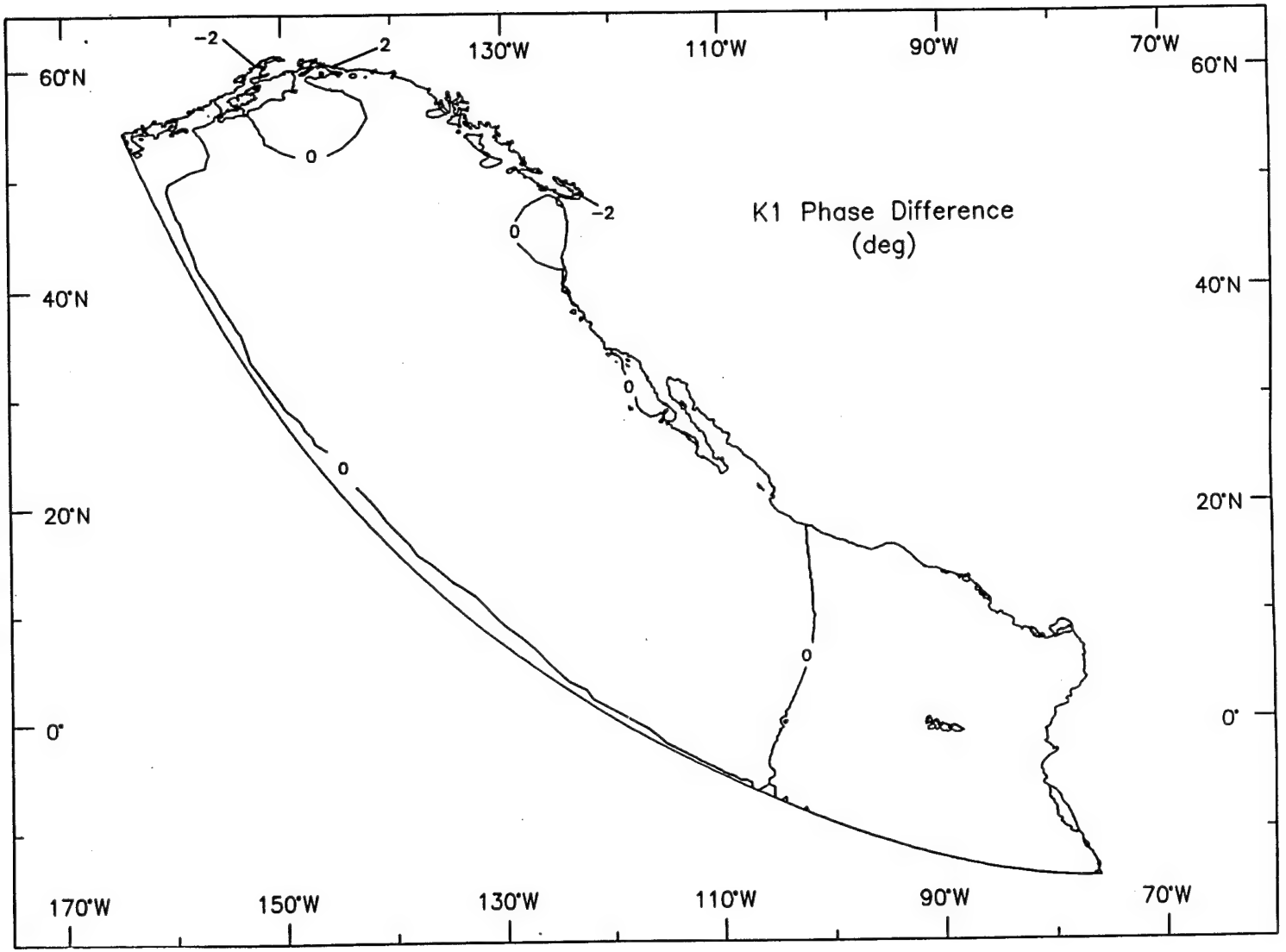

Figure 4. (Sheet 4 of 4)

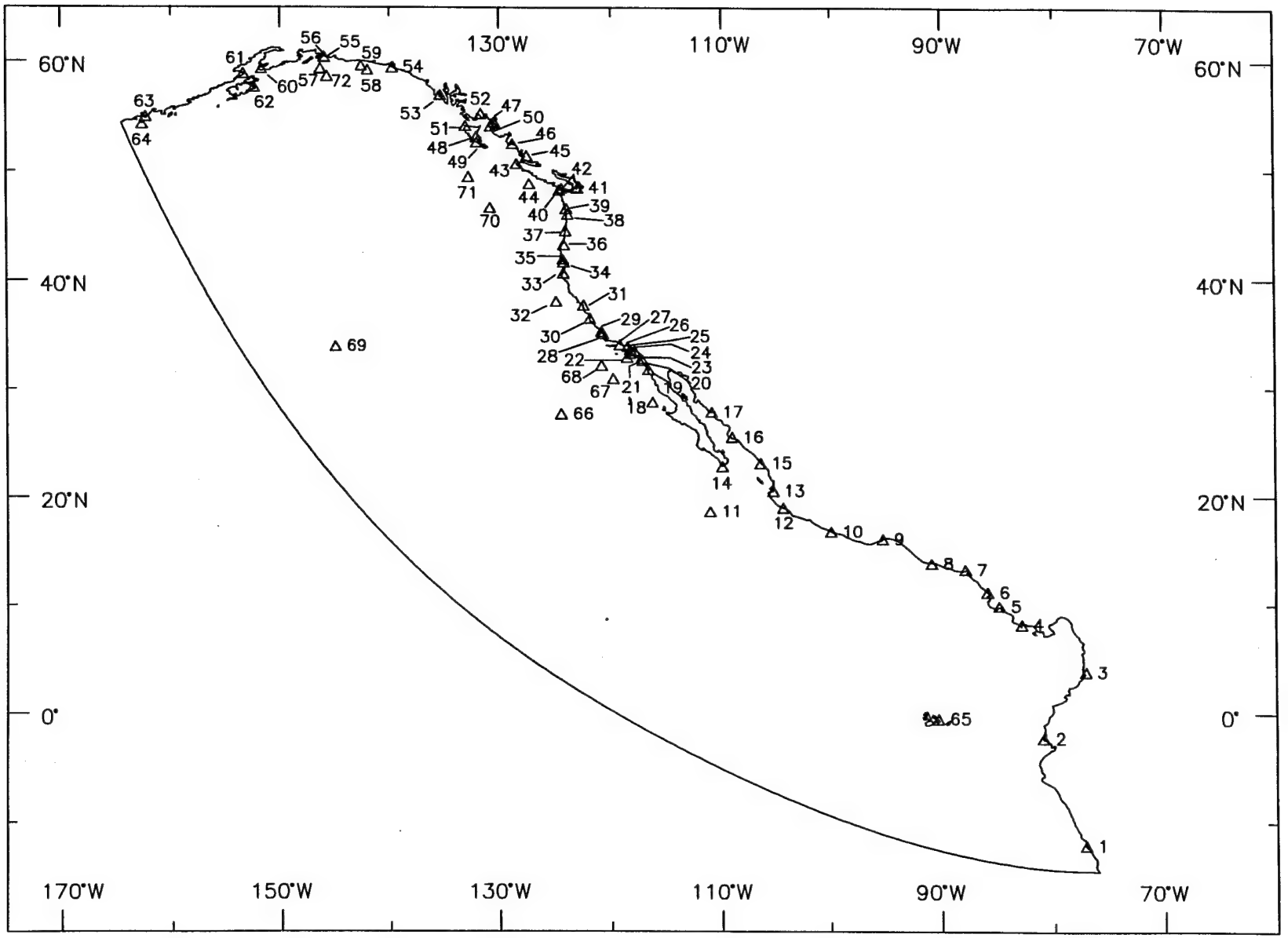

Figure 5. Locations and reference numbers of stations throughout the ENPACT model domain where observed tidal constituents are available.

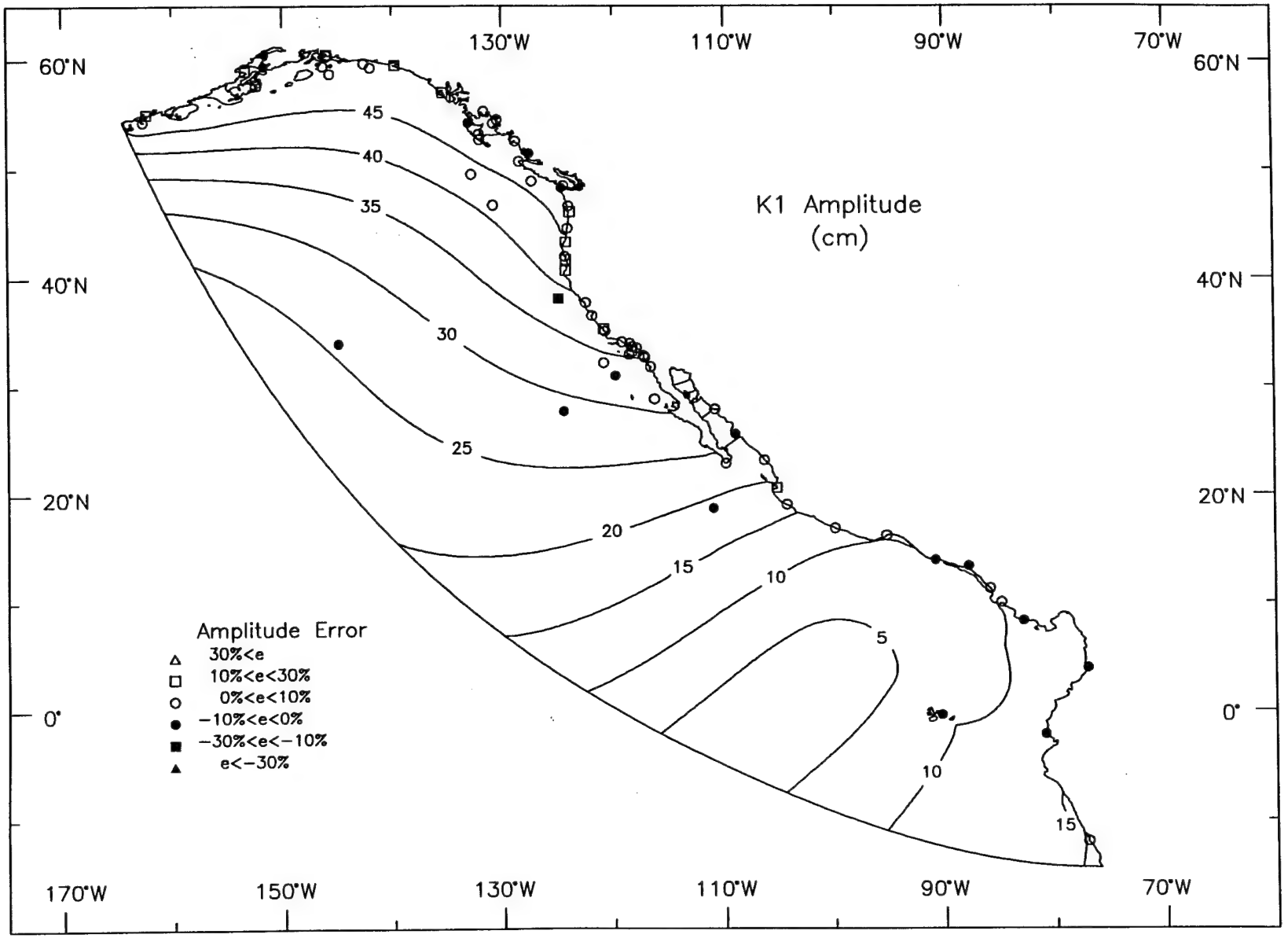

Figure 6. Computed contours for elevation amplitudes (meters) and phases (degrees relative to Greenwich Mean Time) for the two diurnal astronomical tidal constituents used for boundary and interior domain forcing. (Sheet 1 of 4)

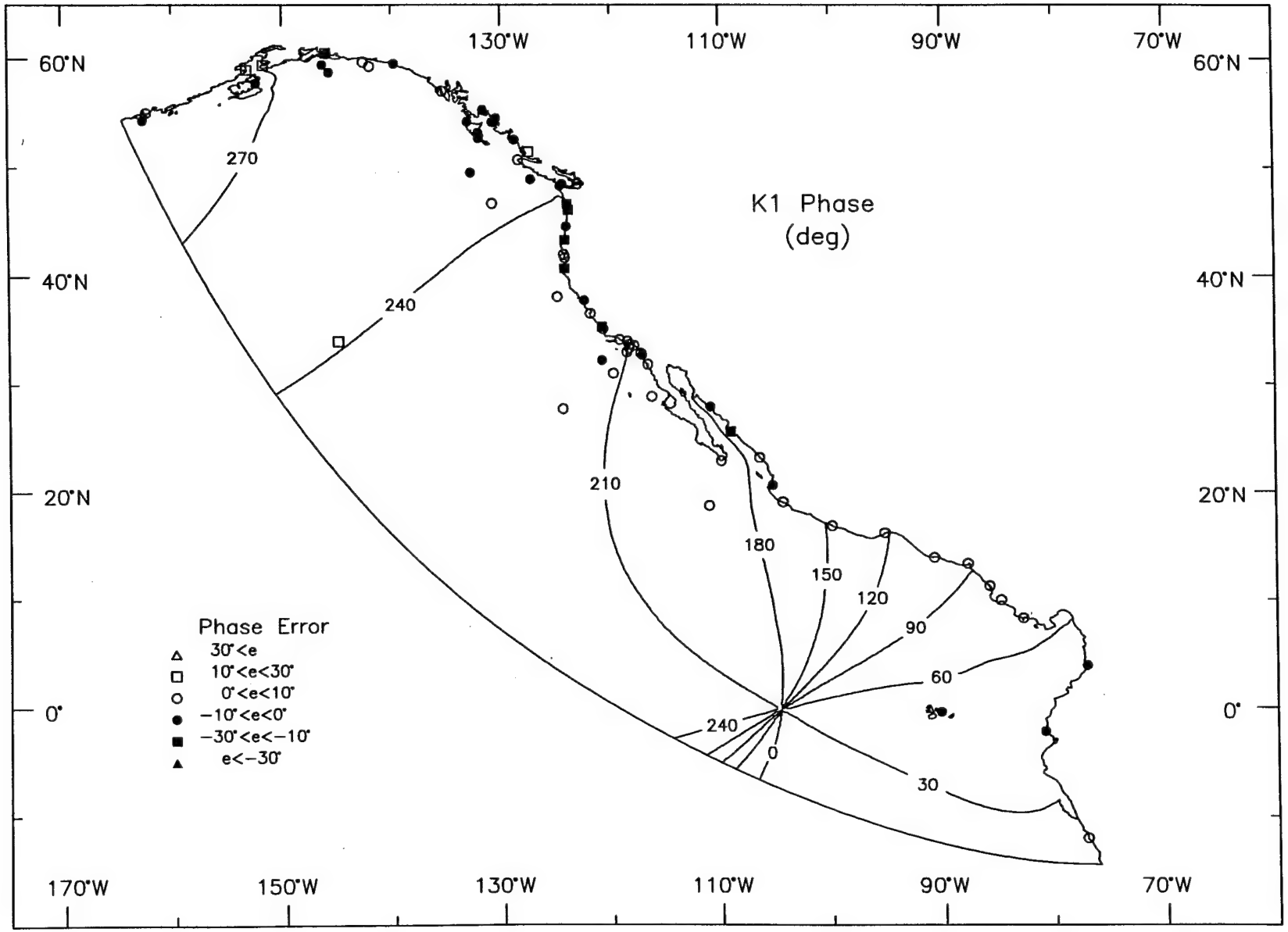

Figure 6. (Sheet 2 of 4)

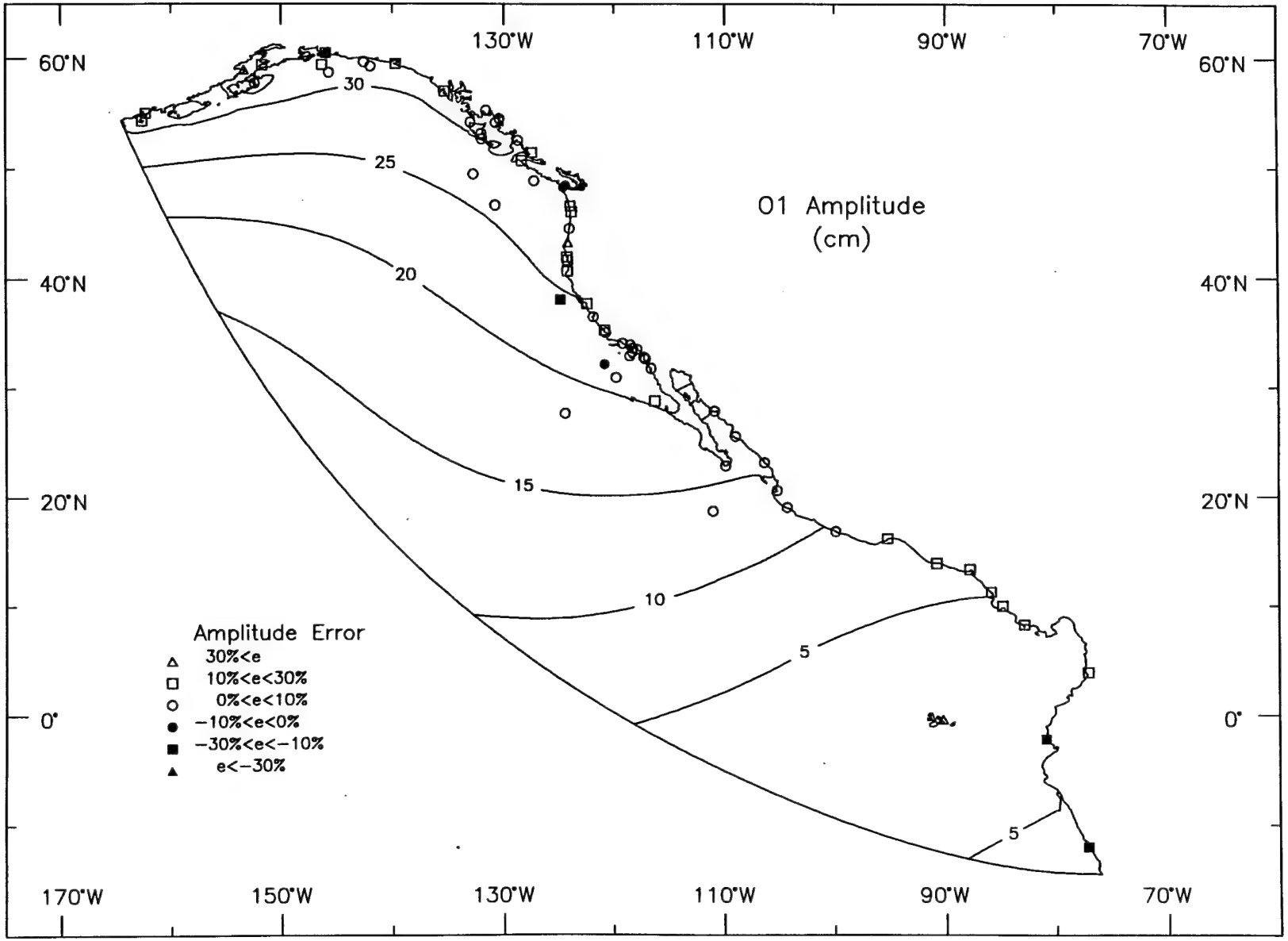

Figure 6. (Sheet 3 of 4)

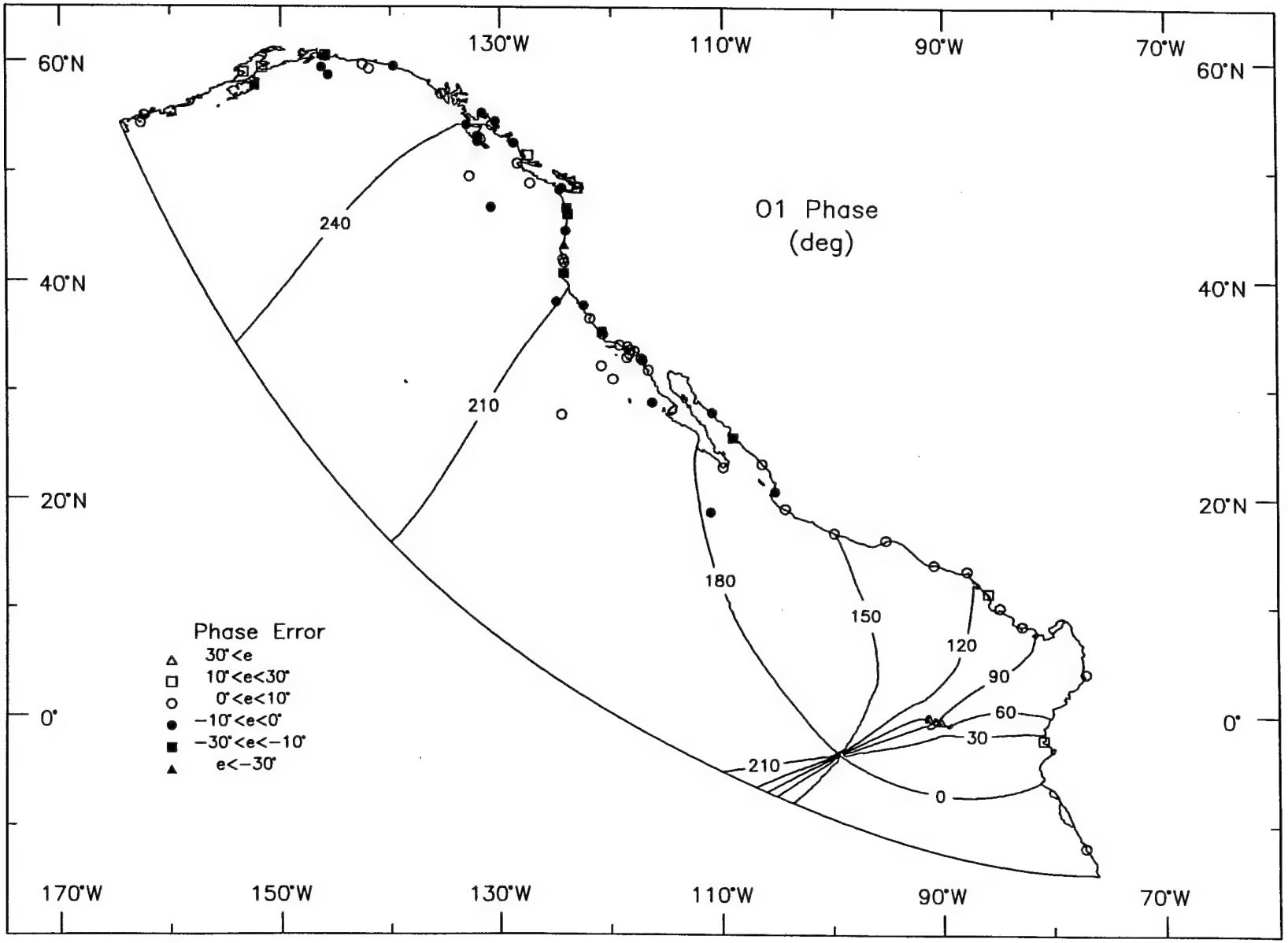

Figure 6. (Sheet 4 of 4)

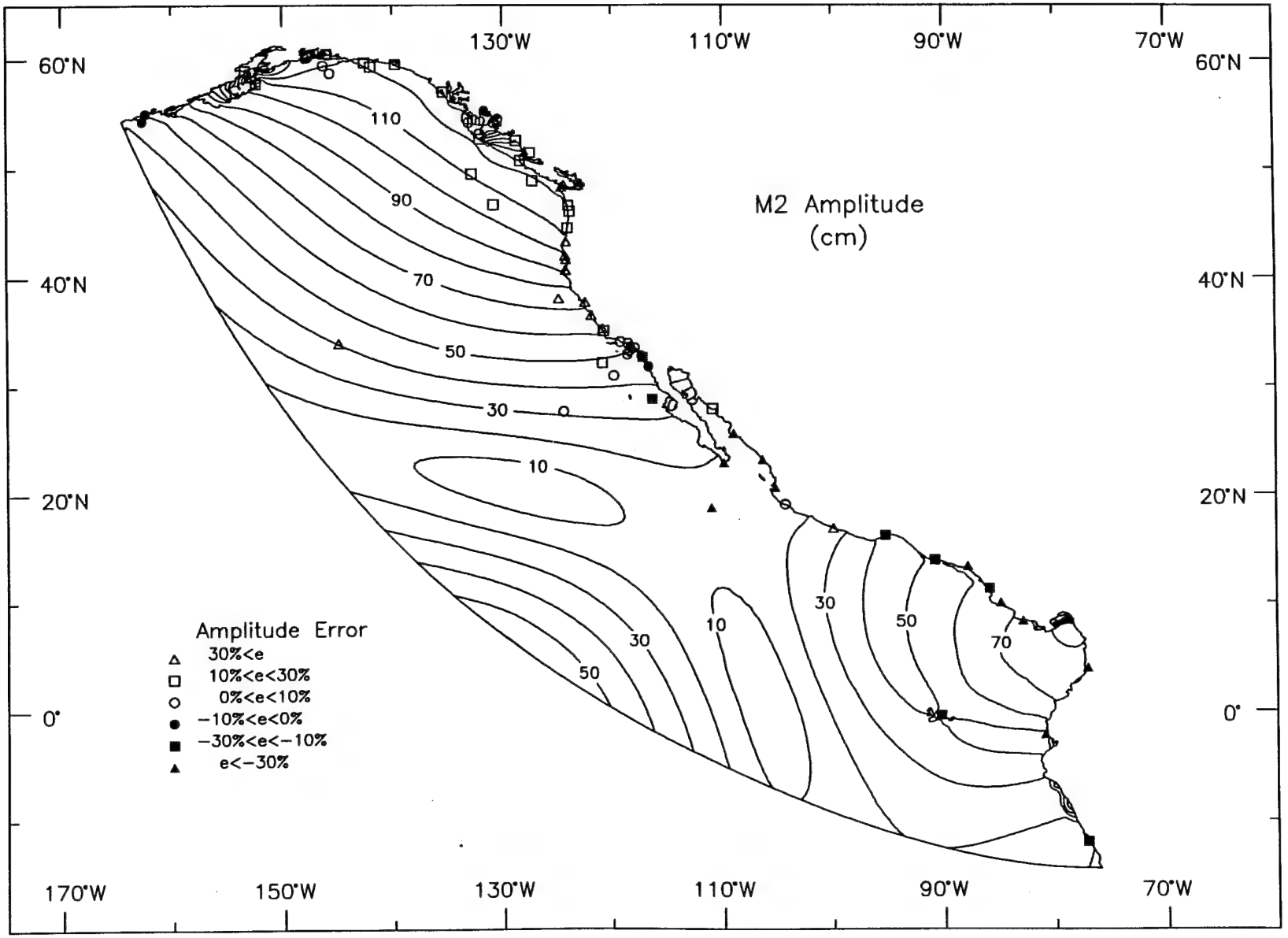

Figure 7. Computed contours for elevation amplitudes (meters) and phases (degrees relative to Greenwich Mean Time) for the three semidiurnal astronomical tidal constituents used for boundary and interior domain forcing. (Sheet 1 of 6)

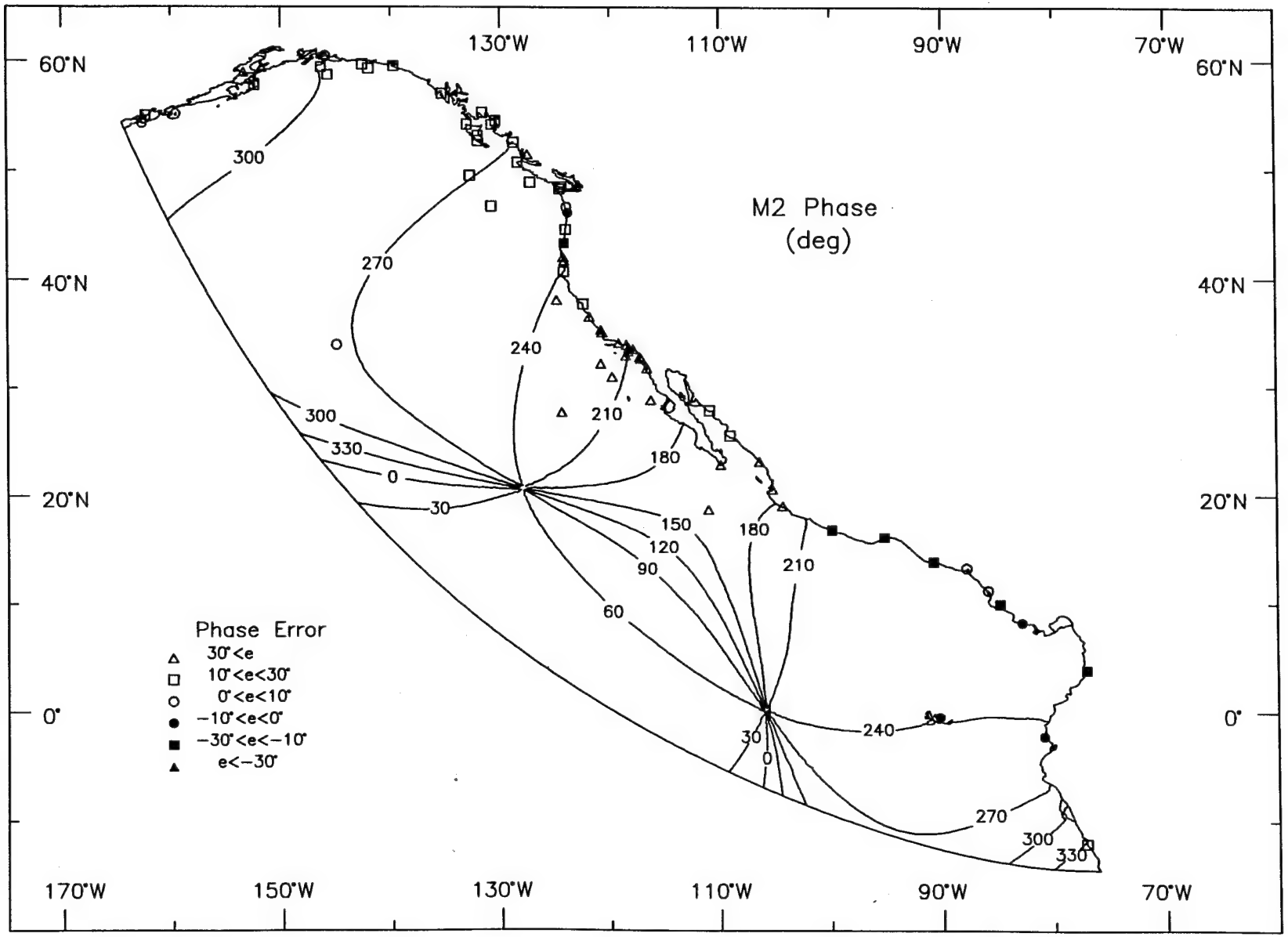

Figure 7. (Sheet 2 of 6)

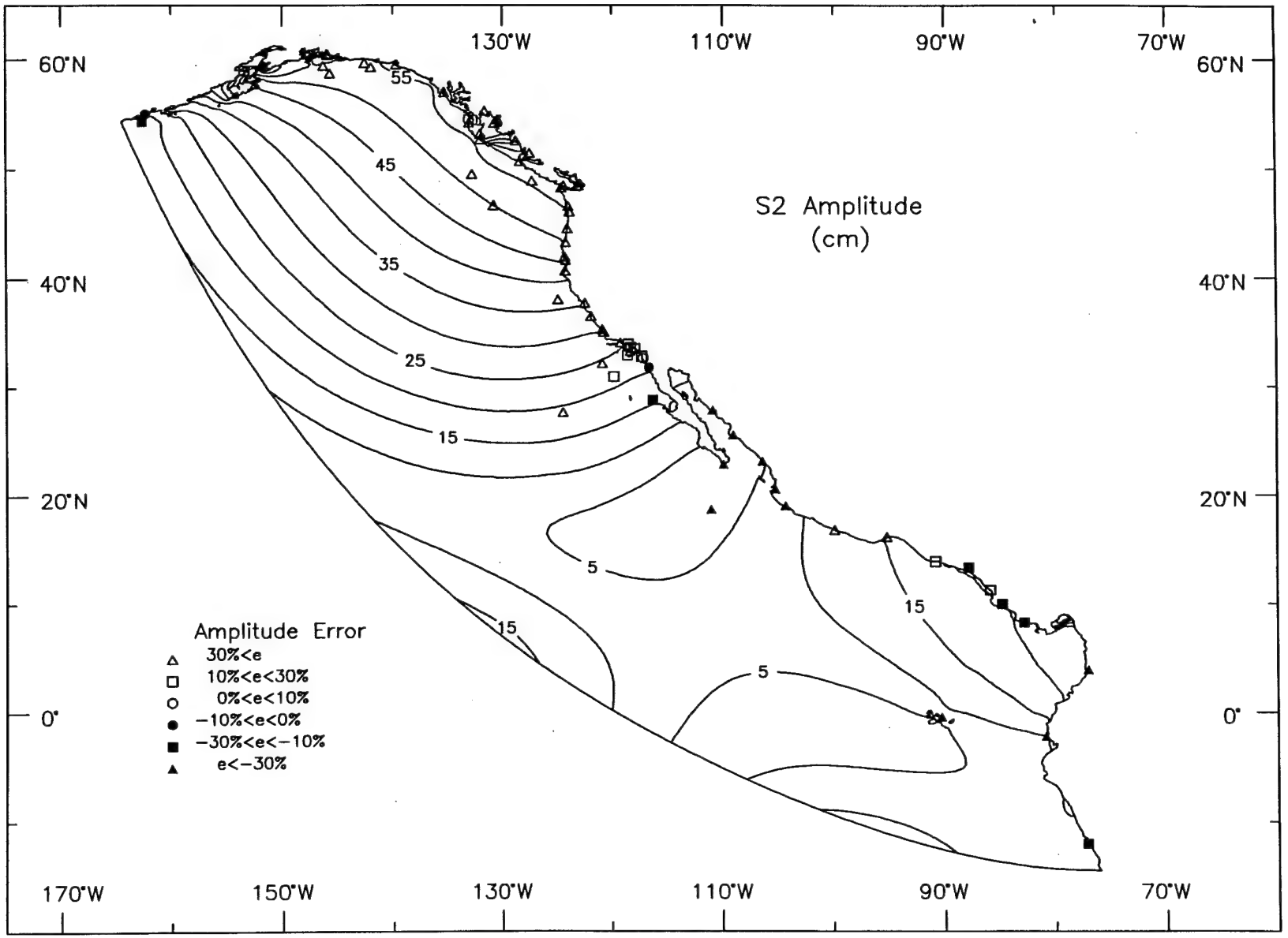

Figure 7. (Sheet 3 of 6)

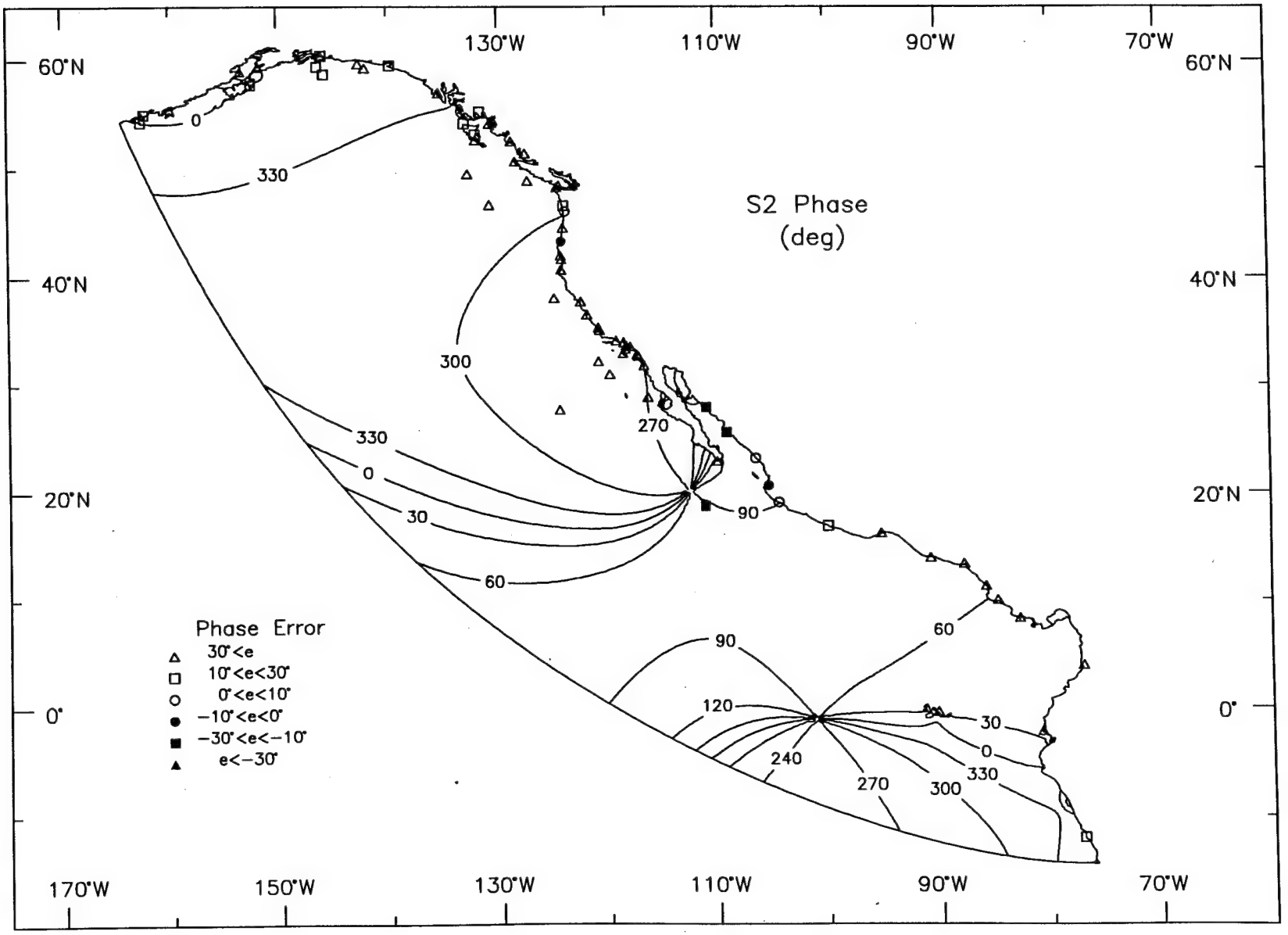

Figure 7. (Sheet 4 of 6)

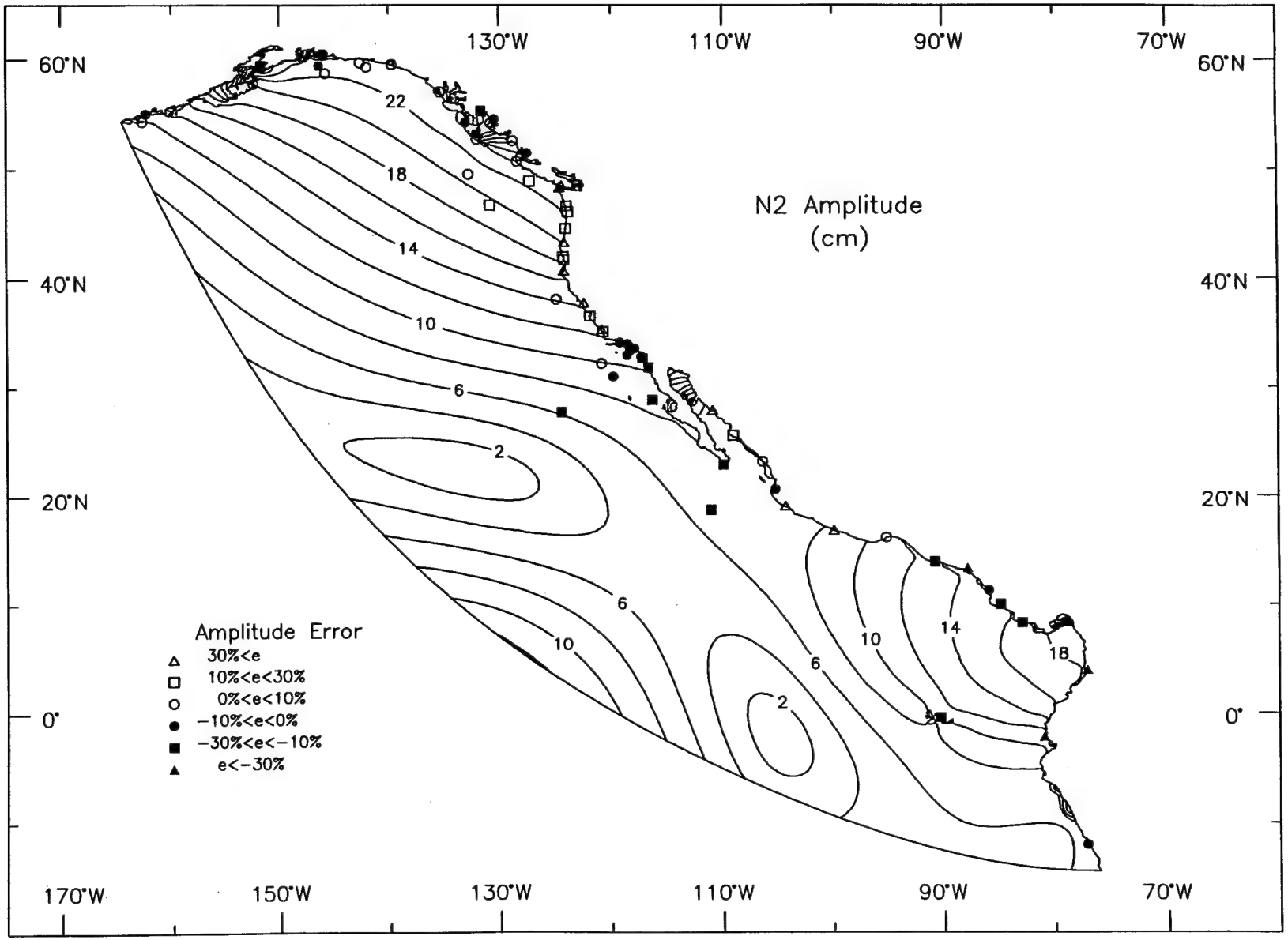

Figure 7. (Sheet 5 of 6)

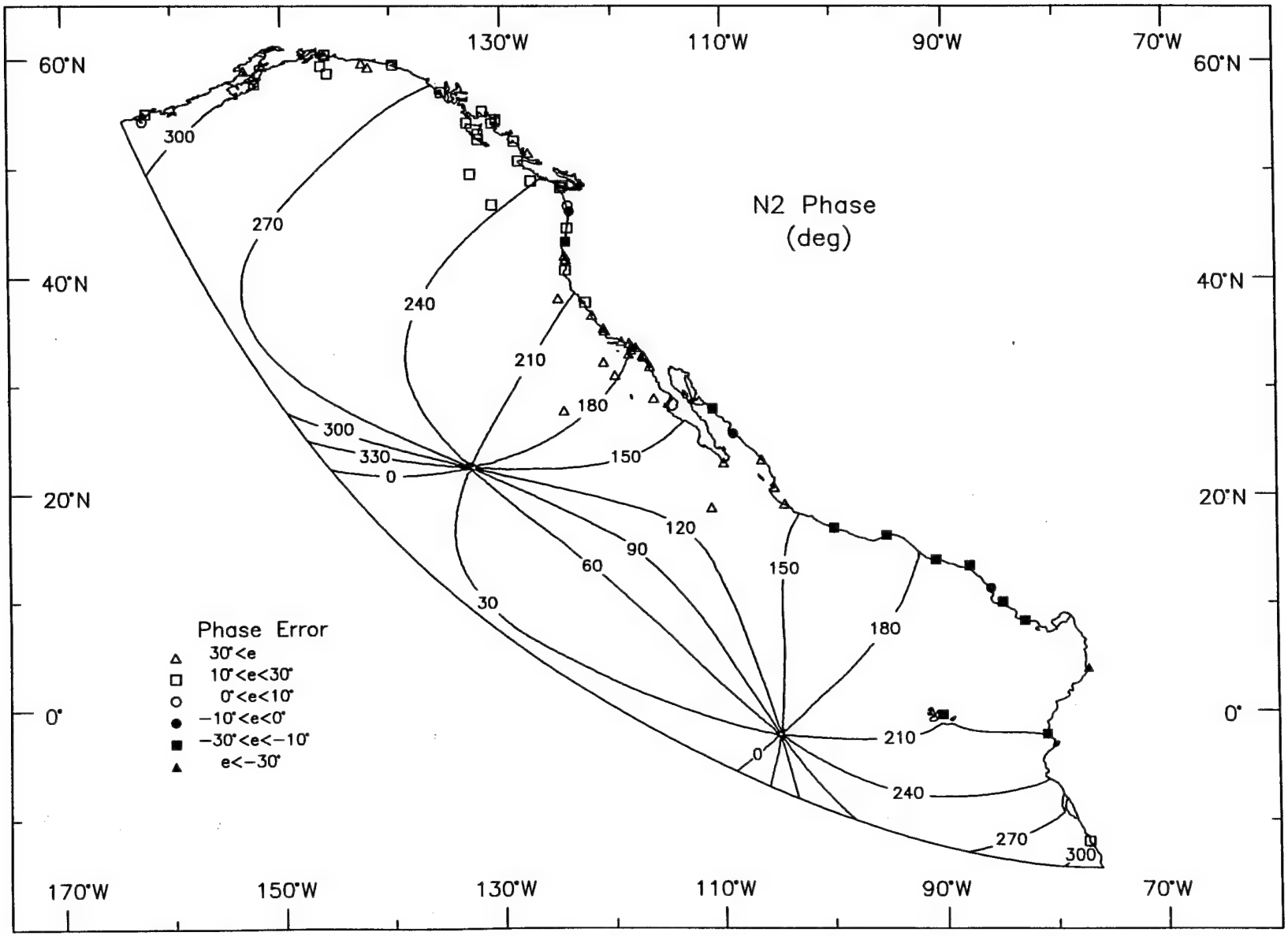

Figure 7. (Sheet 6 of 6)

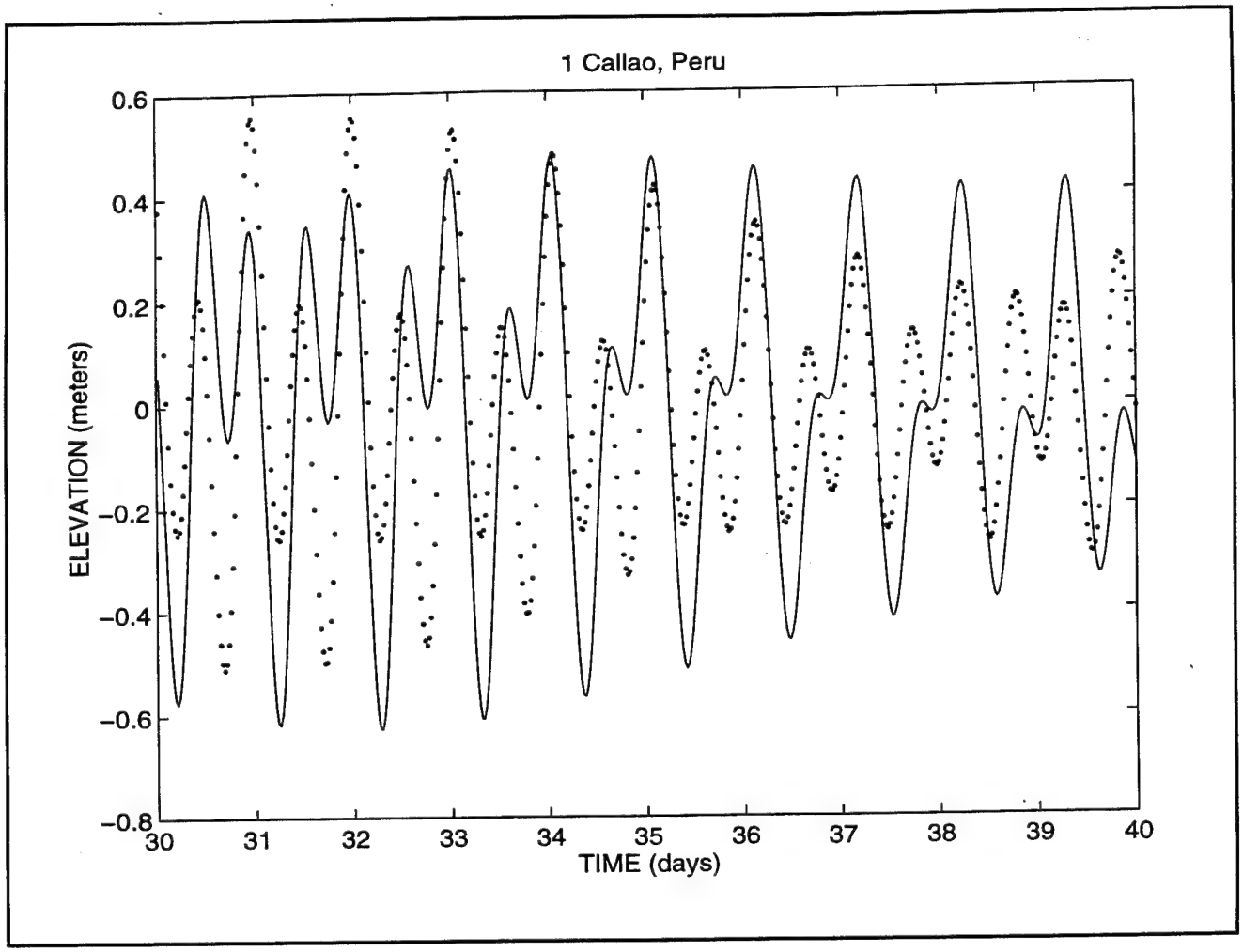

Figure 8. Time histories of surface elevations at representative stations within the ENPACT model domain. These plots have been constructed using the K_1, O_1, M_2, S_2, and N_2 tidal constants from the ENPACT model (solid line) and from observed data (dashed line). (Sheet 1 of 10)

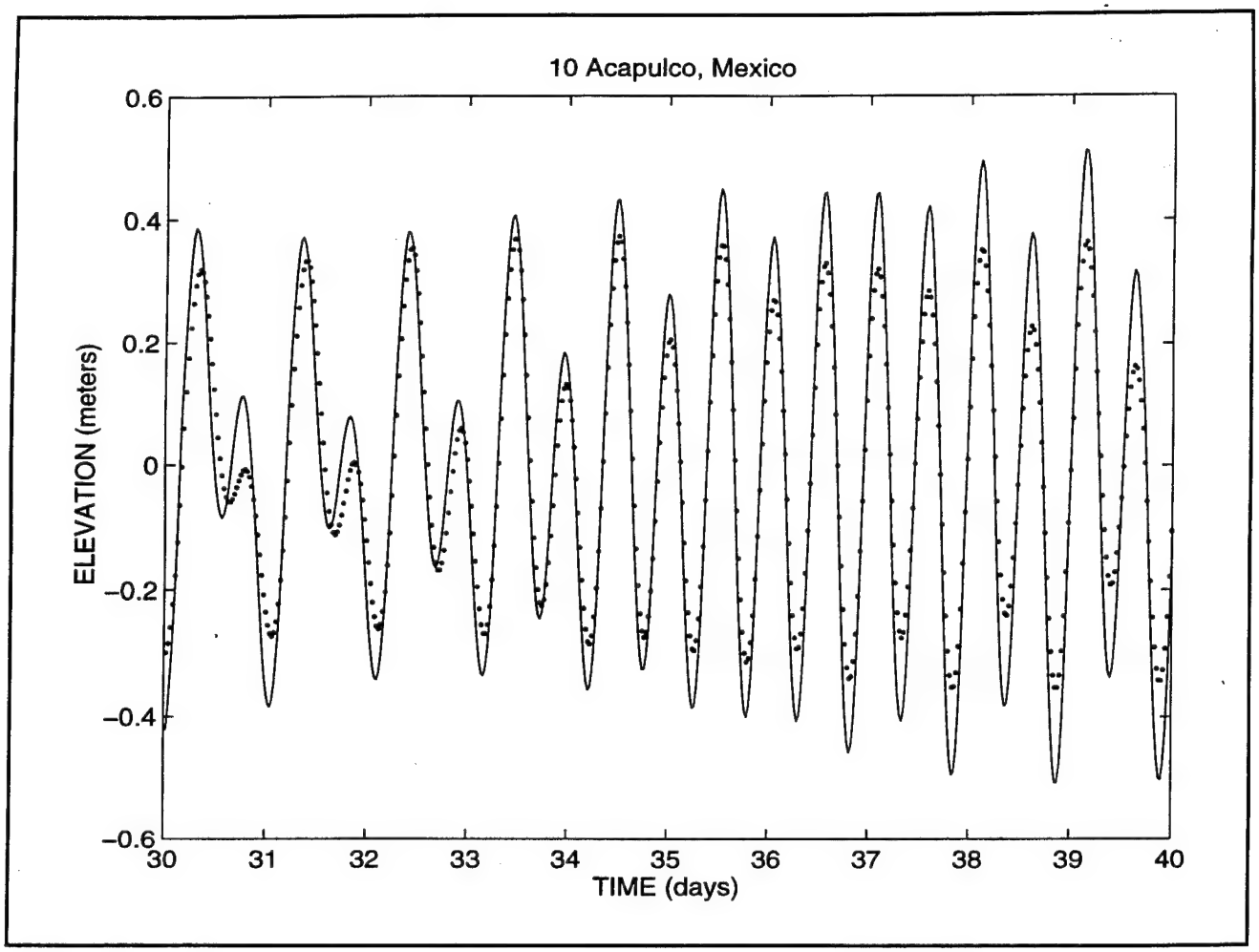

Figure 8. (Sheet 2 of 10)

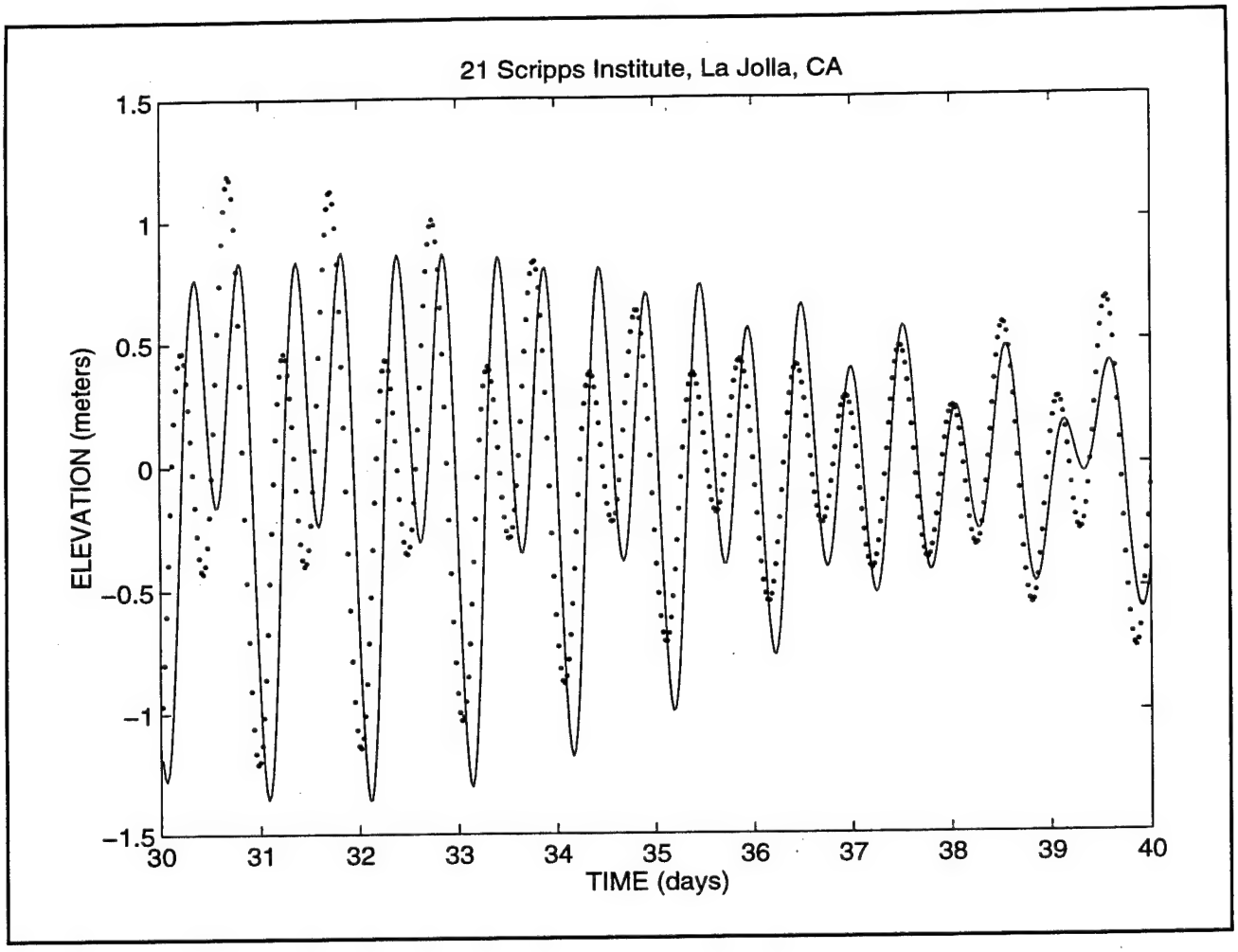

Figure 8. (Sheet 3 of 10)

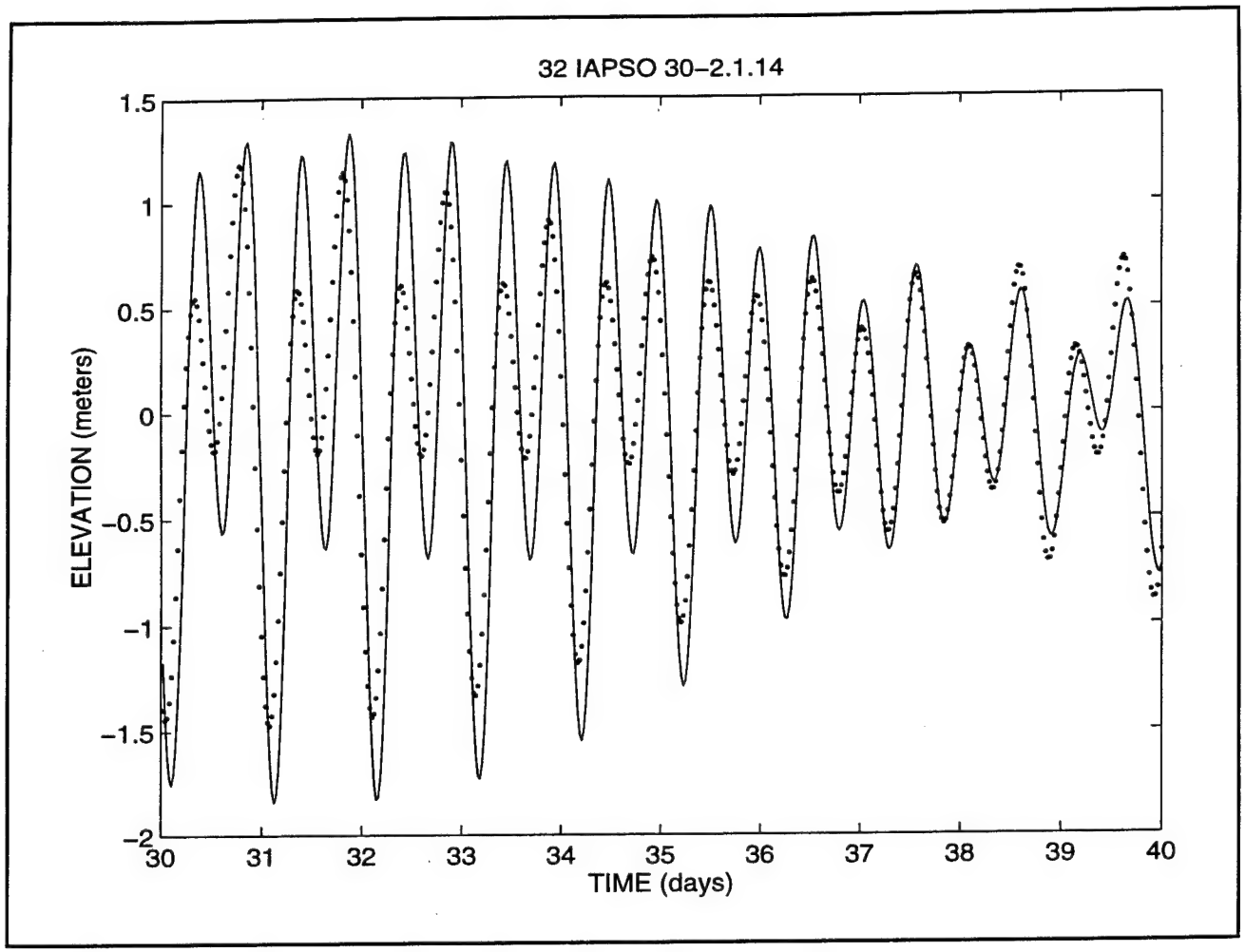

Figure 8. (Sheet 4 of 10)

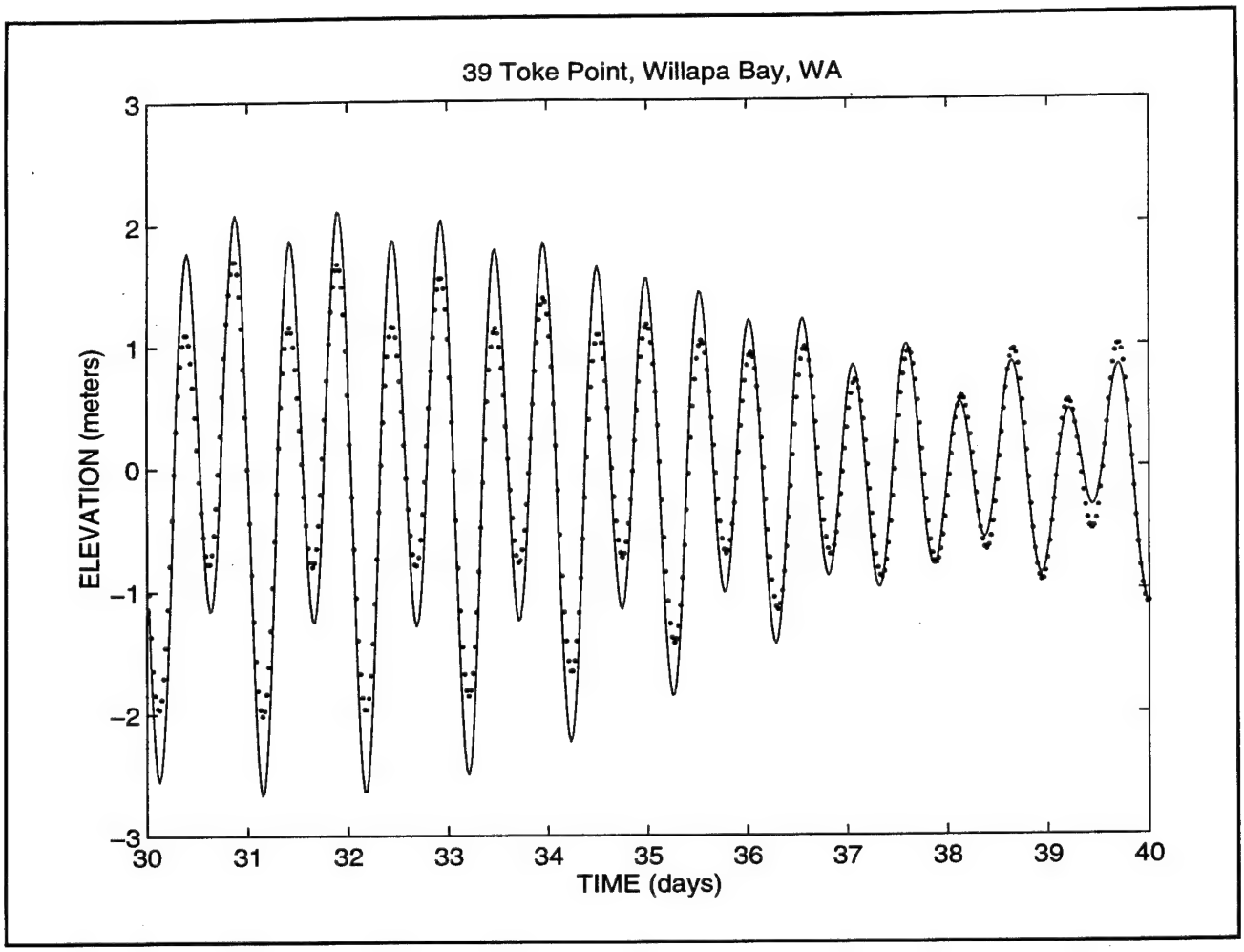

Figure 8. (Sheet 5 of 10)

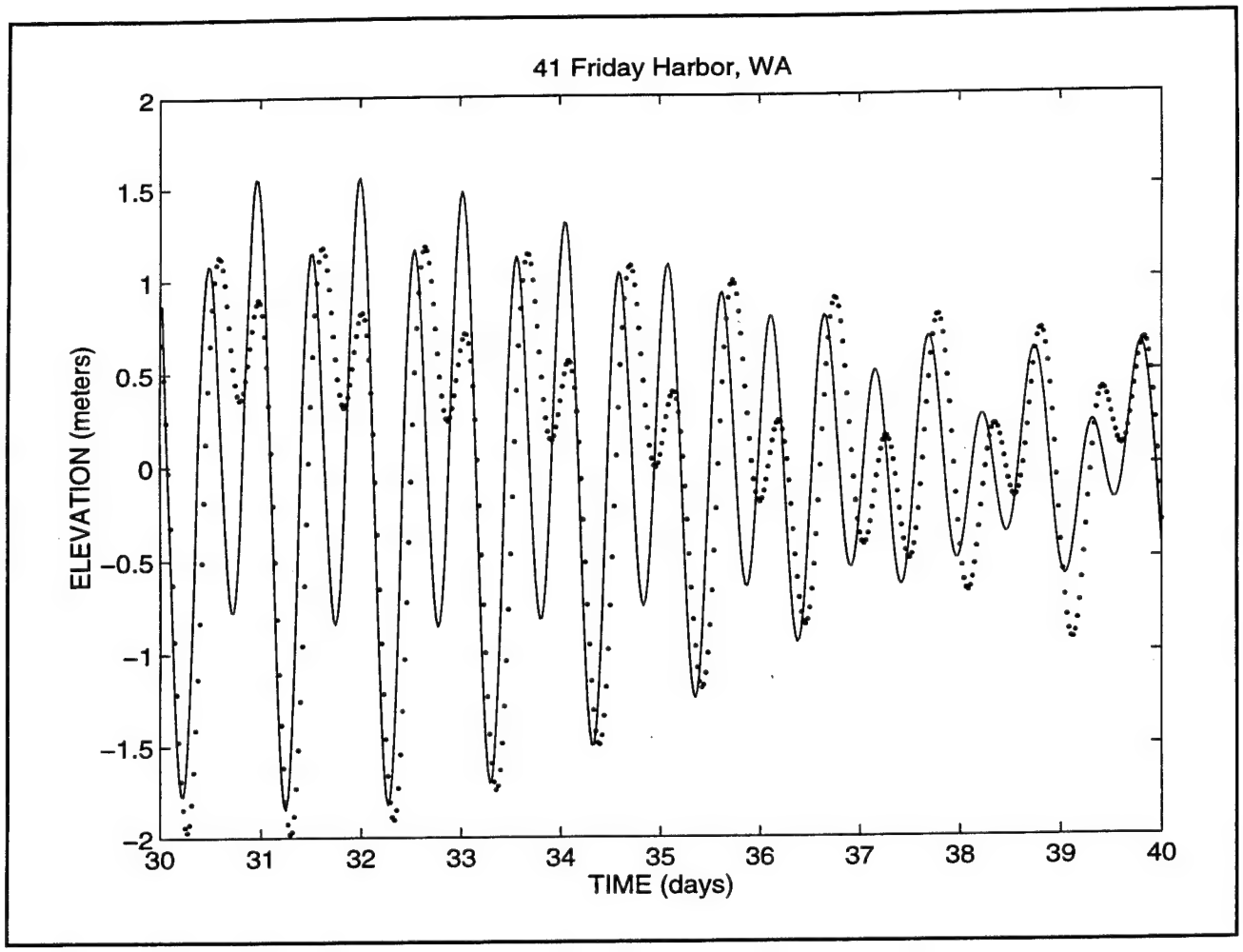

Figure 8. (Sheet 6 of 10)

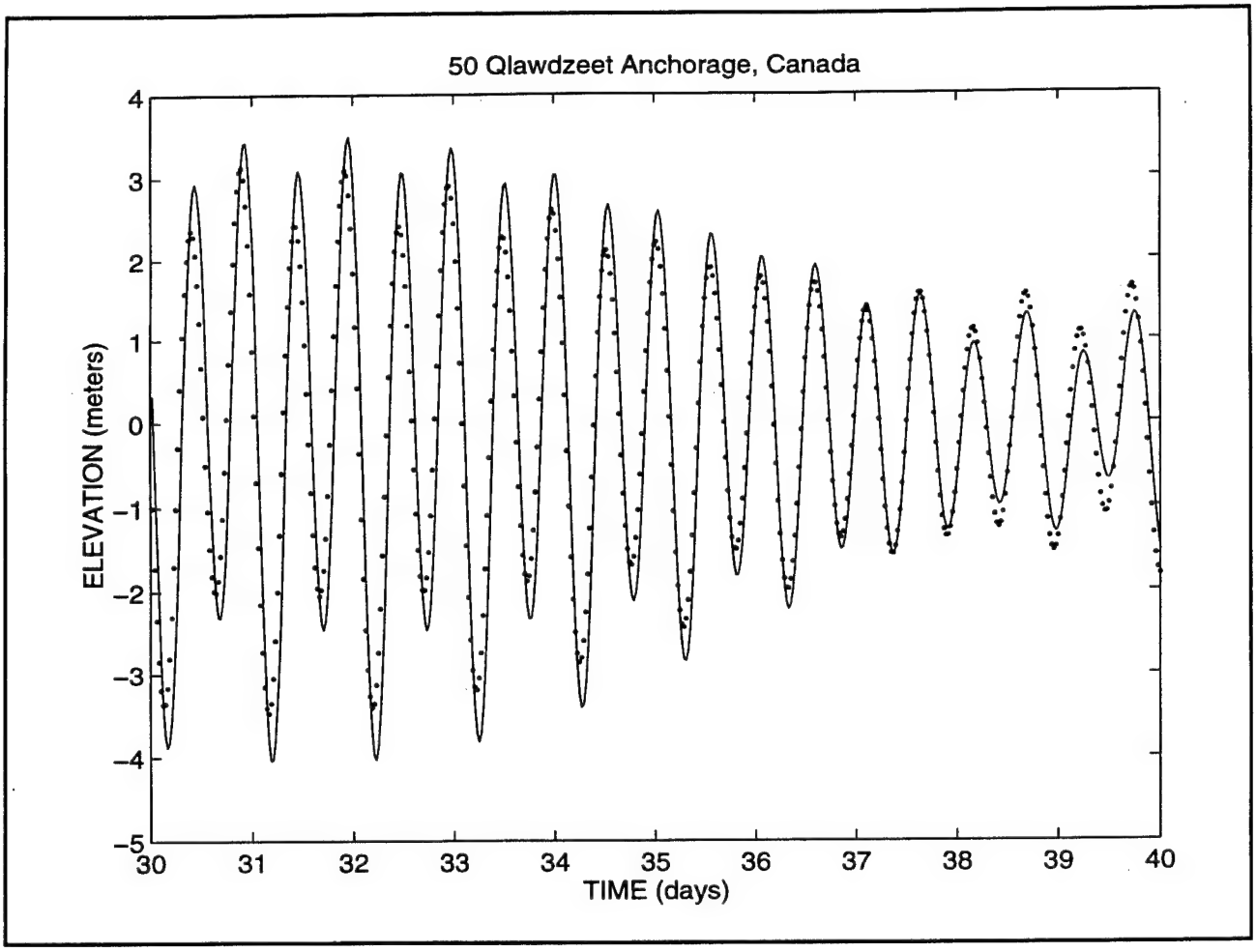

Figure 8. (Sheet 7 of 10)

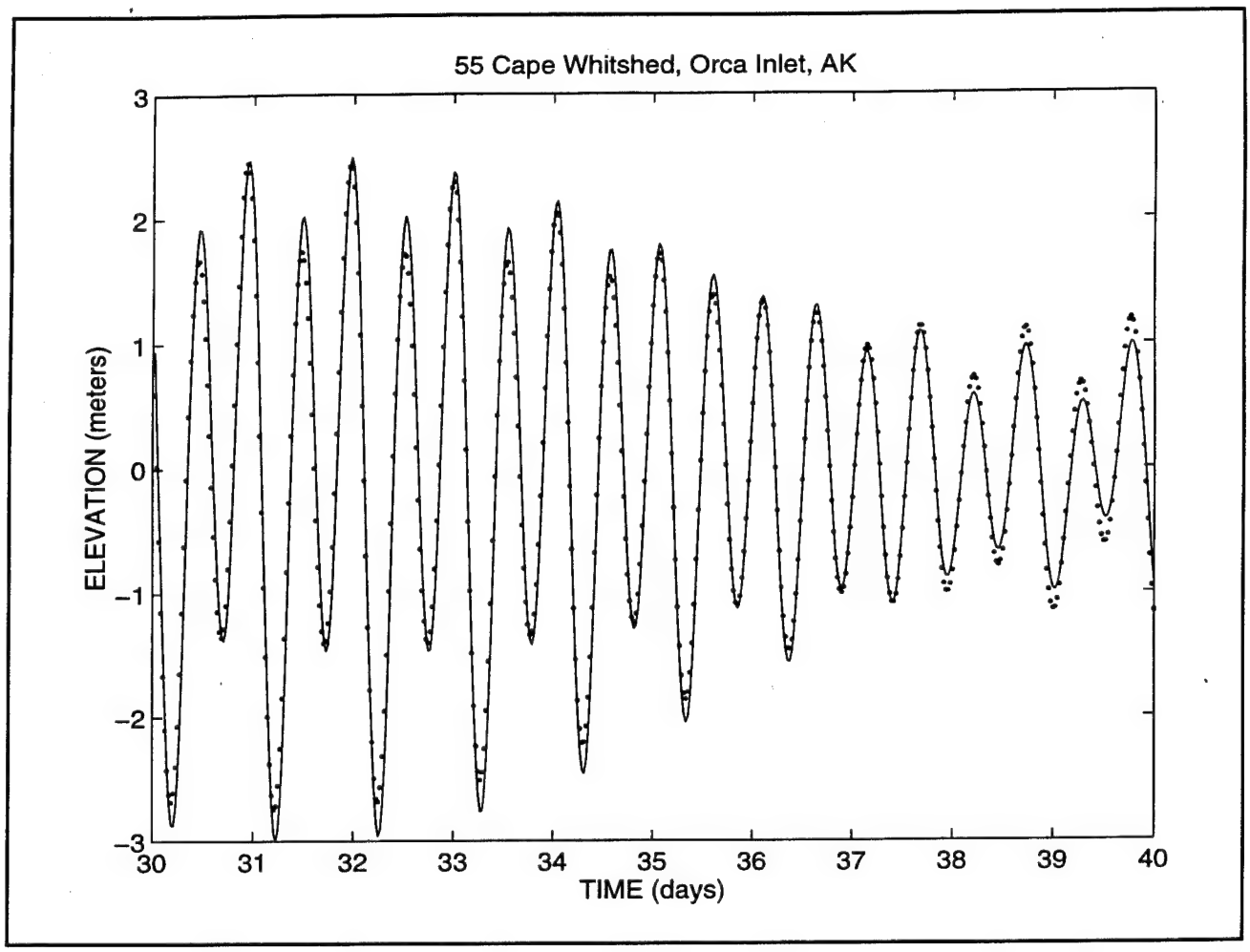

Figure 8. (Sheet 8 of 10)

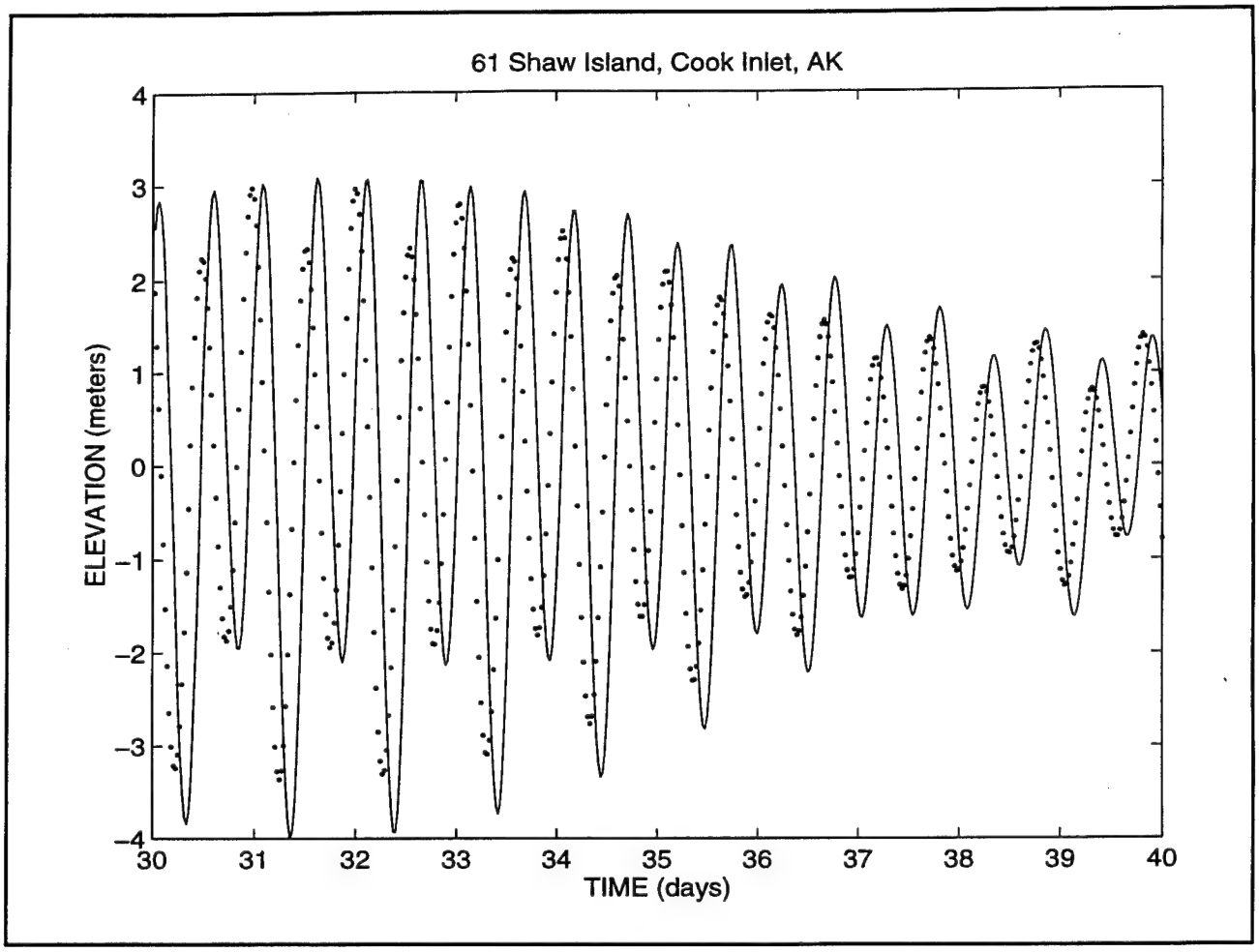

Figure 8. (Sheet 9 of 10)

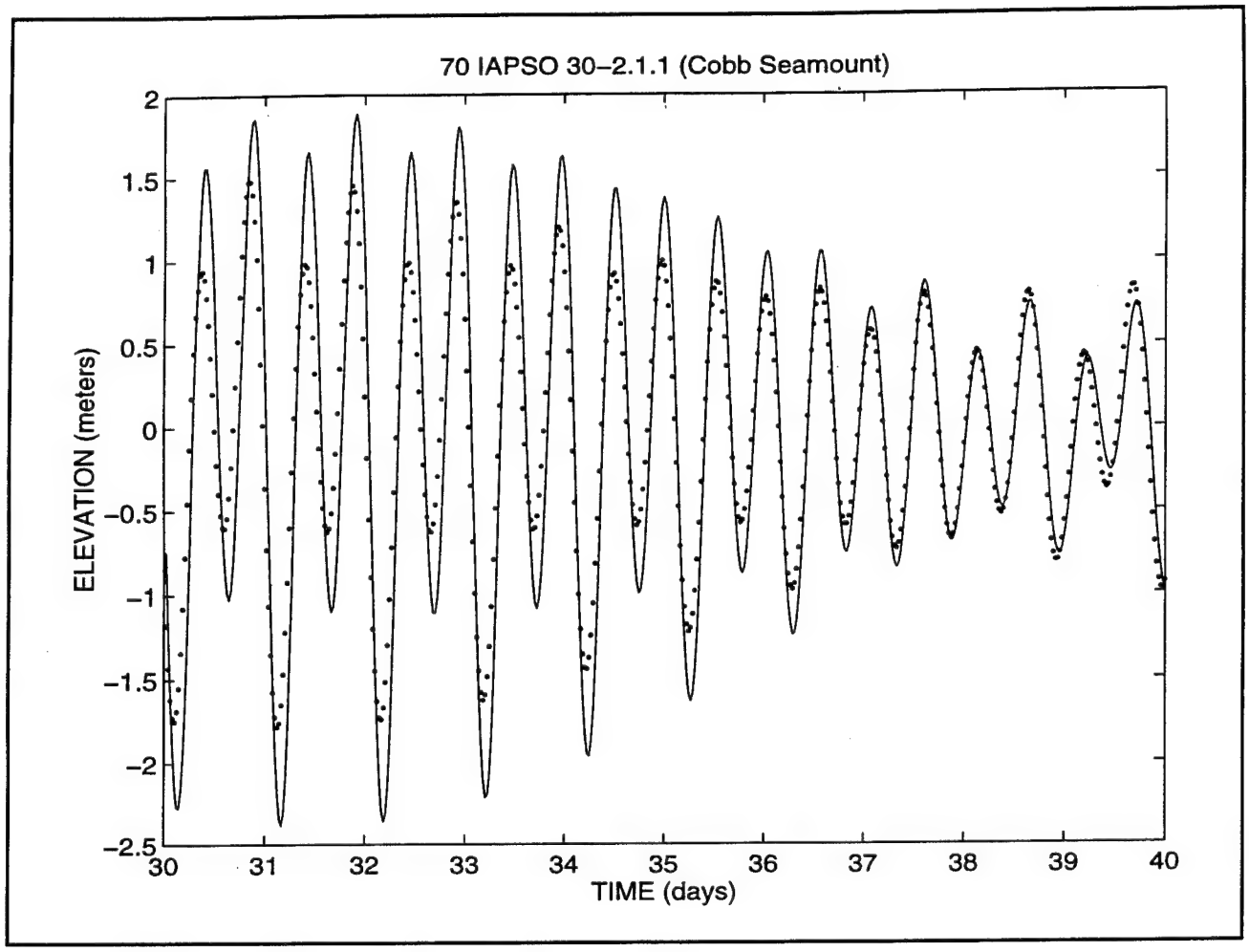

Figure 8. (Sheet 10 of 10)

Table 1
Observational Tidal Elevation Station Locations and Record Durations

Station Number	Station Name	Position (longitude - latitude)	Location	Record Length
1	Callao, Peru	77_9' W - 12_2' S	coast	369 days
2	Port Liberty, Equador	80_55' W - 2_13' S	coast	358 days
3	Buenaventura, Columbia	77_6' W - 3_54' N	coast	369 days
4	Puerto Armuelles, Panama	82_51' W - 8_16' N	coast	369 days
5	Puntarenas, Costa Rica	84_50' W - 9_58' N	coast	369 days
6	San Juan Del Sur, Nicaragua	85_52' W - 11_15' N	coast	369 days
7	La Union (Cutuco), El Salvador	87_49' W - 13_20' N	coast	369 days
8	San Jose, Guatemala	90_49' W - 13_53' N	coast	369 days
9	Salina Cruz, Mexico	95_12' W - 16_10' N	coast	369 days
10	Acapulco, Mexico	99_54' W - 16_50' N	coast	369 days
11	Isla Socorro, Mexico	111_1' W - 18_43' N	coast	369 days
12	Manzanillo, Mexico	104_19' W - 19_3' N	coast	369 days
13	Puerto Vallarta, Mexico	105_14' W - 20_36' N	coast	369 days
14	Cabo San Lucas, Mexico	109_54' W - 22_53' N	coast	369 days
15	Mazatlan, Mexico	106_24' W - 23_11' N	coast	369 days
16	Topolobampo, Mexico	109_2' W - 25_36' N	coast	369 days
17	Guaymas, Mexico	110_54' W - 27_55' N	coast	369 days
18	Isla Guadalupe, Mexico	116_17' W - 28_52' N	coast	369 days
19	Ensenada, Mexico	116_38' W - 31_51' N	coast	369 days
20	San Diego, CA	117_10' W - 32_43' N	coast	2 years
21	Scripps Institute, La Jolla, CA	117_16' W - 32_52' N	coast	369 days
22	Wilson Cove, San Clemente Is., CA	118_33' W - 33_0' N	coast	29 days
23	Avalon, Catalina Island, CA	118_19' W - 33_21' N	coast	29 days
24	Ocean Pier, Balboa, CA	117_54' W - 33_36' N	coast	369 days
25	Outer Harbor, Los Angeles, CA	118_16' W - 33_43' N	coast	3 years
26	Santa Monica, CA	118_30' W - 34_0' N	coast	369 days
27	Port Hueneme, CA	119_12' W - 34_9' N	coast	369 days

(continued)

Source of Tidal Data: International Hydrographic Organization Tidal Constituent Bank (1990)

Table 1 (Continued)

Station Number	Station Name	Position (longitude - latitude)	Location	Record Length
28	Avila, CA	120_44' W - 35_10' N	coast	369 days
29	Morro Bay, CA	120_51' W - 35_22' N	coast	163 days
30	Monterey, CA	121_53' W - 36_36' N	coast	366 days
31	Golden Gate, San Francisco, CA	122_27' W - 37_48' N	coast	11 years
32	IAPSO 30-2.1.14	124_54' W - 38_9' N	shelf	58 days
33	Humboldt Bay, CA	124_14' W - 40_45' N	coast	369 days
34	Crescent City, CA	124_12' W - 41_45' N	coast	369 days
35	Brookings, OR	124_17' W - 42_3' N	coast	369 days
36	Marshfield, Coos Bay, OR	124_13' W - 43_23' N	coast	369 days
37	South Beach, Newport, OR	124_3' W - 44_38' N	coast	365 days
38	Youngs Bay, Astoria, OR	123_51' W - 46_10' N	coast	369 days
39	Toke Point, Willapa Bay, WA	123_58' W - 46_42' N	coast	369 days
40	Neah Bay, WA	124_37' W - 48_22' N	coast	369 days
41	Friday Harbor, WA	123_0' W - 48_33' N	coast	365 days
42	Port Renfrew, Canada	124_25' W - 48_33' N	coast	62 days
43	Cape Scott, Canada	128_25' W - 50_47' N	coast	86 days
44	IAPSO 30-2.1.2	127_17' W - 48_58' N	shelf	18 days
45	Wadhams, Canada	127_31' W - 51_31' N	coast	69 days
46	Milne Island, Canada	128_46' W - 52_37' N	coast	50 days
47	Port Simpson, Canada	130_26' W - 54_34' N	coast	69 days
48	Queen Charlotte, Canada	132_4' W - 53_15' N	coast	62 days
49	Tasu Sound, Canada	132_2' W - 52_45' N	coast	86 days
50	Qlawdzeet Anchorage, Canada	130_46' W - 54_13' N	shelf	87 days
51	Langara Island, Canada	133_3' W - 54' 15' N	coast	39 days
52	Ketchikan, AK	131_38' W - 55_20' N	coast	3 years
53	Sitka, AK	135_20' W - 57_3' N	coast	2 years
54	Yukutat, AK	139_44' W - 59_33' N	coast	369 days
55	Cape Whitshed, Orca Inlet, AK	145_55' W - 60_28' N	coast	29 days
56	Orca Bay, Prince William Sound, AK	146_0' W - 60_32' N	coast	29 days
57	Middleton Island, AK	146_19' W - 59_28' N	coast	29 days

(continued)

Table 1 (Concluded)

Station Number	Station Name	Position (longitude - latitude)	Location	Record Length
58	IAPSO 30-2.1.6	141_59' W - 59_20' N	shelf	145 days
59	IAPSO 30-2.1.5	142_34' W - 59_43' N	shelf	170 days
60	Seldovia, AK	151_43' W - 59_26' N	coast	365 days
61	Shaw Island, Cook Inlet, AK	153_23' W - 59_0' N	coast	29 days
62	Kodiak, AK	152_24' W - 57_47' N	coast	369 days
63	King Cove, AK	162_19' W - 55_4' N	coast	239 days
64	Peterson Bay, Sanak Island, AK	162_38' W - 54_23' N	coast	15 days
65	Baltra Island, Galapagos Islands	90_17' W - 0_26' S	coast	366 days
66	IAPSO 30-2.1.13	124_26' W - 27_45' N	deep ocean	26 days
67	IAPSO 30-2.1.11	119_48' W - 31_2' N	deep ocean	37 days
68	IAPSO 30-2.1.12	120_51' W - 32_14' N	deep ocean	8 days
69	IAPSO 30-2.1.9	145_0' W - 34_0' N	deep ocean	15 days
70	IAPSO 30-2.1.1 (Cobb Seamount)	130_49' W - 46_46' N	deep ocean	203 days
71	Union Seamount	132_47' W - 49_35' N	deep ocean	10 days
72	IAPSO 30-2.1.3	145_43' W - 58_46' N	deep ocean	40 days

Table 2
Range of Amplitude Values for Open Boundary Forcing Obtained from a Global Ocean Model (Le Provost, et al., 1994)

Species, *j*	*n*	Constituent	*Maximum* Amp_{jn}, m	*Minimum* Amp_{jn}, m
1	1	K_1, luni-solar	0.4425	0.0194
	2	O_1, principal lunar	0.2974	0.0063
2	1	M_2, principal lunar	0.6021	0.0932
	2	S_2, principal solar	0.1671	0.0319
	3	N_2, elliptical lunar	0.1218	0.0226

Table 3
Tidal Potential Constants for the Principal Tidal Constituents (from Reid, 1990) and the Associated Effective Earth Elasticity Factor (from Wahr, 1981)

Species, *j*	*n*	Constituent	T_{jn}, hr	C_{jn}, m	α_{jn}
1	1	K_1, luni-solar	23.934470	0.141565	0.736
	2	O_1, principal lunar	25.819342	0.100514	0.695
2	1	M_2, principal lunar	12.420601	0.242334	0.693
	2	S_2, principal solar	12.000000	0.112841	0.693
	3	N_2, elliptical lunar	12.658348	0.046398	0.693

Table 4
Comparison of Amplitude Errors Between Calculated and Observed Values, $E^{calc-obs}_{j-amp}$, for Constituent *j*, in Various Regions of the Domain

		$E^{calc-obs}_{j-amp}$ (see Equation 11)				
j	Constituent	Entire Domain Stations 1 - 72	South and Central America Stations 1 - 19	U.S. West Coast Stations 20 - 41	Canada and Alaska Stations 42 - 64	Offshore Stations 65 - 72
1	K_1	0.153	0.064	0.237	0.085	0.028
2	O_1	0.165	0.088	0.228	0.133	0.033
3	M_2	0.227	0.362	0.338	0.145	0.215
4	S_2	0.655	0.535	1.225	0.531	0.687
5	N_2	0.184	0.299	0.251	0.118	0.149

Table 5
Comparison of Phase Errors Between Calculated and Observed Values, $E^{calc-obs}_{j-phase}$, for Constituent *j*, in Various Regions of the Domain

		$E^{calc-obs}_{j-phase}$ (see Equation 12)				
j	Constituent	Entire Domain Stations 1 - 72	South and Central America Stations 1 - 19	U.S. West Coast Stations 20 - 41	Canada and Alaska Stations 42 - 64	Offshore Stations 65 - 72
1	K_1	5.0	3.4	5.4	6.5	3.7
2	O_1	6.2	4.9	6.1	6.8	8.0
3	M_2	33.7	32.9	40.1	26.4	38.7
4	S_2	66.2	67.9	82.6	40.6	94.6
5	N_2	32.9	27.1	38.4	30.0	41.4

Table 6
Distribution of Amplitude Ratio Error, $R_a = \hat{\eta}_j^{calc}(x_i, y_i) / \hat{\eta}_j^{obs}(x_i, y_i)$, for Constituent *j*, for All Stations within the Domain

j	Const-ituent	Distribution of R_a by Number of Stations												
		R_a < 0.5	0.5 < R_a ≤ 0.6	0.6 < R_a ≤ 0.7	0.7 < R_a ≤ 0.8	0.8 < R_a ≤ 0.9	0.9 < R_a ≤ 1.0	1.0 < R_a ≤ 1.1	1.1 < R_a ≤ 1.2	1.2 < R_a ≤ 1.3	1.3 < R_a ≤ 1.4	1.4 < R_a ≤ 1.5	1.5 < R_a ≤ 2.0	2.0 < R_a
1	K_1	1	0	0	0	1	11	46	10	3	0	0	0	0
2	O_1	1	0	0	0	3	2	38	17	7	3	0	0	0
3	M_2	1	4	5	2	5	5	17	11	9	4	4	5	0
4	S_2	9	1	0	3	3	1	3	4	5	5	4	17	16
5	N_2	0	1	2	5	7	18	18	7	4	4	2	3	0

Table 7
Distribution of Phase Error, $P_d = \varphi_j^{calc}(x_i, y_i) - \varphi_j^{obs}(x_i, y_i)$, for Constituent *j*, for All Stations within the Domain

j	Const-ituent	Distribution of P_d by Number of Stations											
		-180 < P_d < -60	-60 < P_d ≤ -40	-40 < P_d ≤ -30	-30 < P_d ≤ -20	-20 < P_d ≤ -10	-10 < P_d ≤ 0	0 < P_d ≤ 10	10 < P_d ≤ 20	20 < P_d ≤ 30	30 < P_d ≤ 40	40 < P_d ≤ 60	60 < P_d ≤ 180
1	K_1	0	0	0	1	6	26	34	3	2	0	0	0
2	O_1	0	0	1	0	6	21	35	4	3	0	1	0
3	M_2	0	0	0	1	5	4	6	21	6	4	5	20
4	S_2	0	0	1	2	1	2	3	5	8	10	7	32
5	N_2	0	1	1	3	7	3	2	9	15	6	16	7

Appendix A
Resynthesis of Time Histories Using the Cotidal Charts

Resynthesized time histories are useful for examining the general structure of tides and for overall comparisons between model results and observed data. In order to resynthesize a time history from the cotidal charts presented in Figures 6 and 7, the following steps can be applied:

Step 1

Interpolate amplitudes and phases for the five astronomical constituents presented in this report using the most detailed set of cotidal charts available. For example, in order to obtain values for Cape Whitshed, Orca Inlet, AK (located at 145° 55' W and 60° 28' N), the set of cotidal charts presented in Figures 6 and 7 are interpolated. The adjacent amplitudes A_i and Ψ phases can be readily obtained:

Constituent	A_i, m	Ψ_i, deg
K_1	0.504	273
O_1	0.323	256
M_2	1.360	307
S_2	0.619	352
N_2	0.252	287

Step 2

Surface elevations as a function of time can now be computed using the following relationship:

$$\zeta(x,y,t) = \sum_{i}^{5} A_i(x,y) f_i(t_o) \cos\left[\omega_i(t-t_o) + v_i(t_o) - \psi_i^{(radians)}(x,y)\right] \quad \text{(A1)}$$

where

$\zeta(x, y, t)$ = free surface elevation at the site of interest as a function of time

$A_i(x, y)$ = amplitude for the i^{th} constituent

$\Psi_i(x, y)$ = phase for the i^{th} constituent (in radians per second)

$f_i(t_o)$ = nodal factor relative to reference time t_o for the i^{th} constituent

$v_i(t_o)$ = equilibrium argument relative to reference time t_o for the i^{th} constituent

For the five constituents of interest, ω_i has the following values:

Constituent	ω_i, (radians/sec)
K_1	0.000072921158358
O_1	0.000067597744151
M_2	0.000140518902509
S_2	0.000145444104333
N_2	0.000137879699487

Guidelines as to how to compute f_i^{BF} and v_i^{BF} are given by Schureman (1941) and Foreman (1977). If equilibrium tides are computed, f_i^{BF} and v_i^{BF} should be specified as 1.0 and 0.0 for all constituents. A resynthesized signal for the data is presented between 30 and 40 days in Figure A1.

Step 2 (Alternate)

As an alternative to computing a time series according to Equation A1, the constituent tide record generation program in the Automated Coastal Engineering System (ACES) (Leenknecht, Szuwalski, and Sherlock 1990) can be used. This program requires constituent data for the specified location to predict tidal elevations at that locale for a given time period. The tidal constituents contained in this report can be used as input to the ACES program with one modification. The Greenwich epochs Ψ shown in Equation A1 must

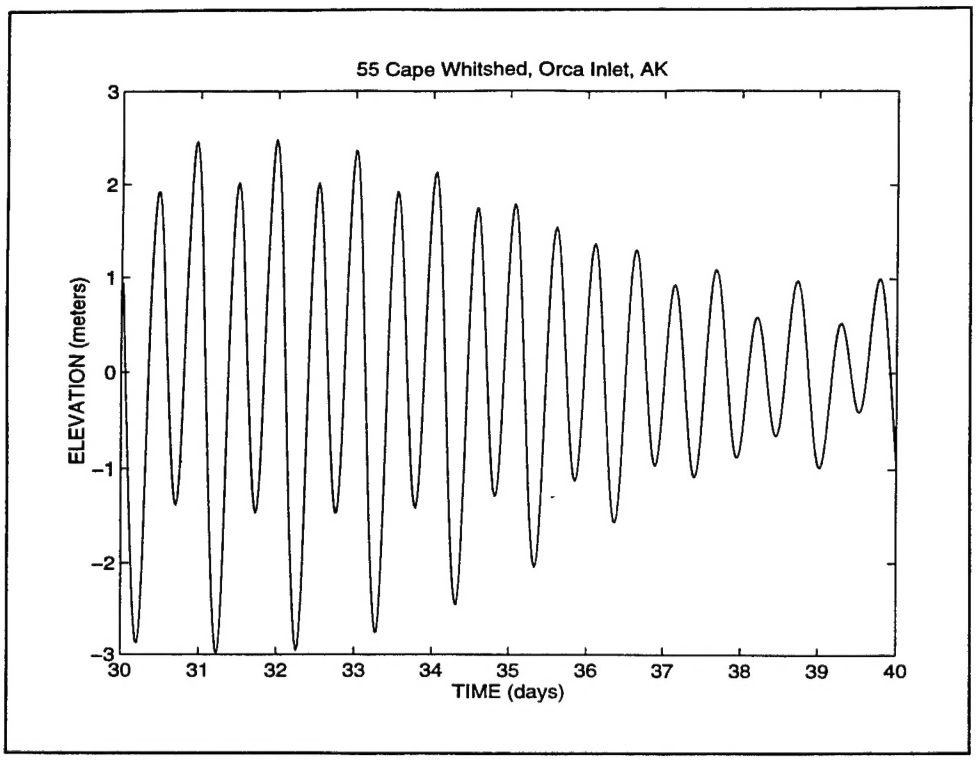

Figure A1. Example time history of resynthesized surface elevations from the K_1, O_1, M_2, S_2, and N_2 tidal constituents at a station in the Eastern North Pacific.

be converted to local epochs κ. This transformation is according to the following relationship:

$$Greenwich\ epoch\ \psi_i = \kappa_i + pL \tag{A2}$$

where κ is the local epoch needed for input to the ACES program to reconstruct a local tide, p is the coefficient of the constituent (i.e., 2 for M_2, 1 for K_i, etc.), and L is the longitude of the location for which a tidal prediction is desired. By making the above adjustment, this report can be used in conjunction with the ACES program to yield tidal predictions at any location along the west coast of the United States, Canada, and Central and part of South America.

Step 3 (Optional)

Comparisons with observational data are often useful in evaluating model accuracy. Observational data available from the International Hydrographic Organization Tidal Constituent Bank and other organizations are sometimes referenced to the epoch of the local station. The following transformation

converts these data to the Greenwich epoch to allow comparisons with ADCIRC results:

$$Greenwich\ epoch\ \psi_i = g_i + a_i \frac{S}{15} \tag{A3}$$

where g_i is the station's local epoch, a_i is the speed of the constituent argument in degrees/hour, and S is longitude of the station's time zone meridian, positive for west and negative for east (Schureman 1941).

Constituent	a_i (deg/hour)
K_1	15.0410686
O_1	13.9430356
M_2	28.9841042
S_2	30.0000000
N_2	28.4397295

REPORT DOCUMENTATION PAGE

Form Approved
OMB No. 0704-0188

1. AGENCY USE ONLY *(Leave blank)*

2. REPORT DATE
December 1994

3. REPORT TYPE AND DATES COVERED
Report 6 of a series

4. TITLE AND SUBTITLE
ADCIRC: An Advanced Three-Dimensional Circulation Model for Shelves, Coasts, and Estuaries; Report 6, Development of a Tidal Constituent Database for the Eastern North Pacific

5. FUNDING NUMBERS
Work Unit No. 32466

6. AUTHOR(S)
J. L. Hench, R. A. Luettich, Jr., J. J. Westerink, and N. W. Scheffner

7. PERFORMING ORGANIZATION NAME(S) AND ADDRESS(ES)
University of North Carolina at Chapel Hill, Morehead City, NC 27514
University of Notre Dame, Notre Dame, IN 46556
USAE Waterways Experiment Station, Coastal Engineering Research Center, 3909 Halls Ferry Road, Vicksburg, MS 39180-6199

8. PERFORMING ORGANIZATION REPORT NUMBER
Technical Report DRP-92-6

9. SPONSORING/MONITORING AGENCY NAME(S) AND ADDRESS(ES)
U.S. Army Corps of Engineers; Washington, DC 20314-1000

10. SPONSORING/MONITORING AGENCY REPORT NUMBER

11. SUPPLEMENTARY NOTES
Available from National Technical Information Service, 5285 Port Royal Road, Springfield, VA 22161.

12a. DISTRIBUTION/AVAILABILITY STATEMENT
Approved for public release; distribution is unlimited.

12b. DISTRIBUTION CODE

13. ABSTRACT *(Maximum 200 words)*

This report describes the application of ADCIRC-2DDI, a two-dimensional depth-averaged barotropic hydrodynamic model, to the eastern North Pacific in order to develop a tidal constituent database. Issues that are emphasized in the development of the Eastern North Pacific Tidal (ENPACT) model include the specification of a geometrically and hydrodynamically simple open boundary, the use of large domains, and the advantages of using a graded finite element grid to selectively resolve flow features of interest.

The ENPACT model is coupled to a finite element global ocean model at the open boundary and forced with five diurnal and semidiurnal astronomical tidal constituents (K_1, O_1, M_2, S_2, and N_2). Tidal potential forcing is applied to the interior of the domain for the same constituents. The structures of the various tides are examined and the results of the tidal simulations are compared with field data at 72 fixed tidal elevation stations.

14. SUBJECT TERMS
Circulation model
Eastern North Pacific
Finite element method
Hydrodynamic model
Tidal database
Two-dimensional model

15. NUMBER OF PAGES
60

16. PRICE CODE

17. SECURITY CLASSIFICATION OF REPORT	18. SECURITY CLASSIFICATION OF THIS PAGE	19. SECURITY CLASSIFICATION OF ABSTRACT	20. LIMITATION OF ABSTRACT
UNCLASSIFIED	UNCLASSIFIED		

Destroy this report when no longer needed. Do not return it to the originator.